Institut für Veterinärbiochemie und Molekularbiologie der
Vetsuisse-Fakultät Universität Zürich

Direktor: Prof. Dr. med. vet. Ulrich Hübscher

Involvement of PARP1 in NF-κB-dependent gene expression during the cell cycle

Inaugural-Dissertation

zur Erlangung der Doktorwürde der
Vetsuisse-Fakultät Universität Zürich

vorgelegt von

Sandra Manuela Bäckert

Tierärztin
von Riehen/BS

Genehmigt auf Antrag von
Prof. Dr. med. vet. et phil. II Michael O. Hottiger, Referent
Prof. Dr. med. vet. Hanspeter Nägeli, Koreferent

Zürich, 2009

Table of content

Summary

Acute inflammation is triggered by a variety of cellular stresses and leads among other things to the activation of the nuclear transcription factor kappa B (NF-κB). NF-κB belongs to a family of inducible transcription factors and plays a crucial role in the regulation of many genes involved in mammalian immune and inflammatory response, including cytokines, cell adhesion molecules, complement factors, and a variety of immune receptors. It was shown, that several transcriptional co-factors are involved in the expression of NF-κB target genes. Poly(ADP-ribose) polymerase 1 (PARP1) is a nuclear enzyme converting NAD+ into poly(ADP-ribose) polymers which are attached to PARP1 itself or other proteins. A pathophysiological role of PARP1 has been demonstrated in a number of diseases and animal models, including LPS-induced septic shock. Recently our laboratory provided strong evidence that PARP1 acts as transcriptional co-factor in NF-κB transcriptional activation.

The aim of this thesis was to shed light on the physiological role of PARP1 as transcriptional co-factor for NF-κB-dependent gene expression during the cell cycle.

RAW 267.4 macrophages were transduced with a retrovirus expressing either a shPARP1 or a shMock RNA construct to stably knockdown PARP1 protein levels. Gene expression analyses of several LPS-induced NF-κB-target genes in these cell lines revealed that PARP1 has a dual function. PARP1 acts as co-repressor for Csf2, IL-1b and IL-12 gene expression which is not influenced by cell cycle synchronization. Interestingly, PARP1 acts in unsynchronized cells for the IP-10 gene expression as transcriptional co-activator, but as co-repressor in early S phase (Thymidine or Aphidicolin treated cells). In contrast, PARP1 acts in unsynchronized cells for Mpa2l gene expression as co-repressor, but as co-activator during S phase (cells treated with Thymidine and release). Finally, in unsynchronized cells, gene expression for Lif is PARP1 independent, while after Thymidine (early S phase) and Nodocazol (G2/M) treatment PARP1 acts as co-activator, thus providing evidence that PARP1 can indeed change its function during the cell cycle.

Together our results provide strong evidence for the involvement of PARP1 in NF-κB-dependent gene expression during the cell cycle, although the mechanisms regulating these processes have to be further elucidated. A better understanding of the NF-κB physiology and of factors influencing the expression of NF-κB target genes is of great importance, since NF-κB has been implicated in different cellular processes and in a broad range of diseases, one example being LPS induced septic shock.

Zusammenfassung

Eine akute Entzündung kann durch eine Vielzahl von zellulären Stresssituationen ausgelöst werden und führt unter anderem zur Aktivierung des nukleären Transkriptionsfaktors kappa B (NF-κB). NF-κB gehört zu einer Familie von induzierbaren Transkriptionsfaktoren und spielt eine entscheidende Rolle in der Genregulation von Immun- und Entzündungsreaktionen. Insbesondere die Regulierung von Cytokinen , Zelladhesionsmolekülen, Komplementfaktoren und von etlichen Immunrezeptoren ist von NF-κB reguliert. Poly(ADP-ribose) Polymerase 1 (PARP1) ist ein nukleäres Enzym, welches NAD+ zu Poly(ADP-ribose) Polymeren umwandelt, die sich dann an PARP1 selber oder an andere Proteine anlagern. PARP1 wurde eine pathophysiologische Rolle in mehreren Krankheits- und Tiermodellen zugeschrieben, wie zum Beispiel bei LPS induziertem septischem Schock. PARP1 besitzt eine von den vielen transkriptionellen Kofaktorfunktionen im NF-κB Signalweg.

Das Ziel dieser Dissertation war es, die physiologische Rolle von PARP1 als transkriptioneller Kofaktor in der Genexpression während des NF-κB Signalweges in Abhängigkeit vom Zellzyklus besser zu verstehen.

RAW 267.4 Makrophagen wurden mit einem Retrovirus, welcher entweder ein shPARP1 oder ein shMock RNA Konstrukt exprimiert, transduziert, um die PARP1 Protein Levels entscheidend herabzusetzten. Zellzyklus abhängige Untersuchungen von verschiedenen LPS induzierten NF-κB Zielgenen in asynchronen Zellen zeigen eine "Doppelfunktion" für PARP1. Unabhängig vom Zellzyklus ist PARP1 ein Korepressor für IL-1b, Csf2 und IL-12. Interessanterweise ist für die Genexpression von IP-10 PARP1 ein Koactivator in asynchronene Zellen, aber in der frühen S Phase (mit Thymidin oder Aphidicolin behandelte Zellen) agiert PARP1 als Korepressor. Gegenteilig dazu agiert PARP1 während der Genexpression von Mpa2l als Korepressor in asynchronene Zellen, aber während der S Phase (Zellen behandelt mit Thymidin und Release) spielt PARP1 eine Koactivator Rolle. Für Lif ist die Genexpression in asynchronen Zellen unabhänging von PARP1, jedoch zeigt sich für Zellen mit einer Thymidin (frühe S Phase) Behandlung und einer Nocodazol (G2/M Phase) Behandlung eine Koaktivator Funktion für PARP1. Diese Daten deuten sehr darauf hin, dass PARP1 seine Funktion während des Zellzyklus ändern kann.

Zusammengefasst liefern uns diese Resultate einen eindeutigen Hinweis, dass PARP1 eine zellzyklus abhängige regulatorische Aktivität im NF-κB Signalweg besitzt. Um den exakten Regulationsmechanismus zu verstehen, sind jedoch weitere Studien nötig. Ein besseres Verständnis der NF-κB Physiologie und der beteiligten Kofaktoren, welche die Expression von NF-κB Zielgenen beeinflussen, ist von grosser Bedeutung, da NF-κB bei vielen Krankheitsmechanismen beteiligt ist, wie zum Beispiel bei LPS induziertem septischem Schock.

Abbreviations

ADP	Adenosine diphosphate
AIF	Apoptosis inducing factor
AMD	Auto modification domain
ARD	Ankyrin repeat domain
ATP	Adenosine triphosphate
BRCT	BRCA1 C-terminus
CDK	Cyclin dependent kinase
C-terminus	Carboxy terminus
DBD	DNA binding domain
DNA	Deoxyribonucleic acid
DSB	Double strand break
FACS	Fluorescence activated cell sorting
H1	Histone 1
H2B	Histone 2B
IκB	Inhibitor κB
IKK	IκB kinase
IL	Interleukin
iNOS	Inducible nitric oxide synthase
LPS	Lipopolysaccharide
LZ	Leucin zipper
MAPK	Mitogen-activated protein kinase
MEF	Mouse embryonic fibroblast
NAD	Nicotinamide adenine dinucleotide
NF-κB	Nuclear transcription factor κB
NLS	Nuclear localization signal
N-terminal	Amino terminus
p53	Tumor protein 53
PAMPs	Pathogen-associated molecular patterns
PAR	Poly(ADP-ribose) polymer
PARG	Poly(ADP-ribose) glycohydrolase
PARP	Poly(ADP-ribose) polymerase
PARP1(-/-)	PARP1 knockout

PBS	Phosphate bufferd saline
PI	Propidium iodid
RNA	Ribonucleic acid
SDS	Sodium-dodecyl-sulfate
SSB	Single strand break
TBS	Tris bufferd saline
TBS-T	Tris bufferd saline Tween 20
TLR	Toll like receptor
TNFα	Tumor necrosis factor α
ZF	Zinc finger

1 Introduction

1.1 Nuclear factor kappa B (NF-κB)

1.1.1 Introduction

Nuclear factor kappa B (NF-κB) belongs to a family of inducible transcription factors and regulates gene expression in response to a variety of extracellular and intracellular stimuli (1). NF-κB was initially identified as a biochemical protein capable of binding to a 10 base pairs (bp) sequence within the transcriptional enhancer of the immunoglobulin (Ig) κ light chain gene in B cells (2). NF-κB plays a crucial role in the regulation of many genes involved in mammalian immune and inflammatory response, including cytokines, cell adhesion molecules, complement factors, and a variety of immune receptors (2). It has additionally been implicated as an important regulator of cellular processes such as apoptosis, cell proliferation and differentiation (3). Furthermore, NF-κB plays important roles in a myriad of physiological and pathophysiological scenarios.

1.1.2 The NF-κB family

The mammalian NF-κB family consists of five members; RelA (p65), RelB, c-rel, p105/p50 (NF-κB1) and p100/p52 (NF-κB2). NF-κB is composed of homo- and heterodimers formed by these subunits (4). The family members share a conserved 200-amino acid region within their amino termini, termed the Rel homology domain. This domain is responsible for DNA binding, dimerization, nuclear translocation, and interactions with heterologous transcription factors (5).

1.1.3 NF-κB signalling pathway

In unstimulated cells, NF-κB is sequestered in the cytoplasm as an inactive transcription factor complex through physical association with one of the inhibitors of NF-κB (IκB). The family of IκBs includes IκBα, IκBβ, IκBγ, IκBε, p105/p50 (C terminus), P100/p52 (C terminus), IκB-R, and Bcl-3 (6, 7). Treatment of cells with extracellular stimuli, including cytokines such as IL-1 or TNFα, viral proteins, bacterial LPS, phorbal ester, UV and γ-irridiation or potent oxidants leads to the induction of NF-κB (2, 7). The key regulatory

event for the induction of NF-κB is the phosphorylation of the IκB proteins by the IκB kinase (IKK) complex, which leads to IκB protein ubiquitylation and subsequent degradation (8). This results in the release of cytoplasmic NF-κB complexes, which subsequently translocate to the nucleus where the NF-κB dimers bind to κB sites of target genes (Fig. 1).

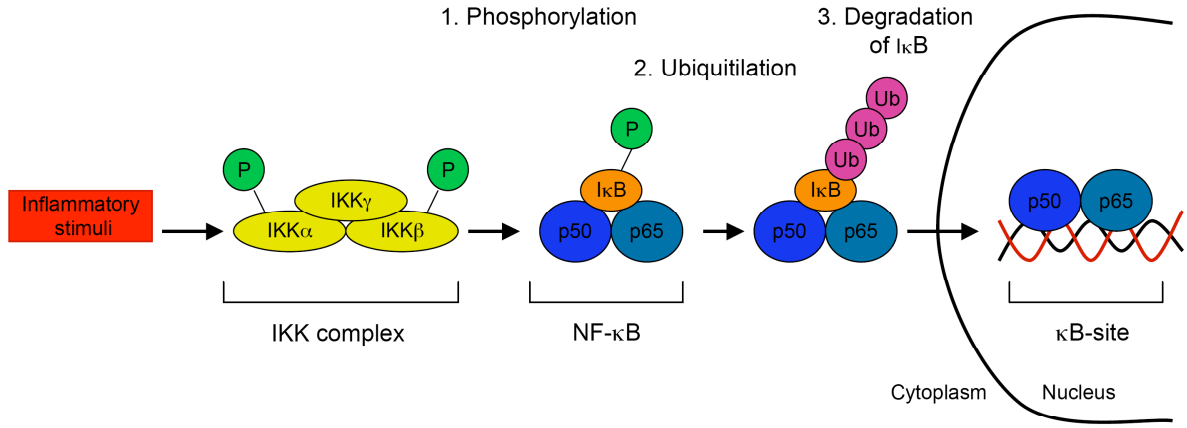

Figure 1: Relevant regulatory nodes in NF-κB signalling pathway. In the simplest model of NF-κB induction, an inflammatory stimulus activates signal transduction pathways that induce the activation of the IKK (inhibitor of NF-κB (IκB) kinase) complex. This results in the phosphorylation and ubiquitylation of IκB proteins and consequently their degradation by the proteasome. Released NF-κB dimers translocate to the nucleus and bind κB-sites in the promoters or enhancers of target genes, which leads to their transcription (8).

Two major signalling pathways have been described and characterized so far which result in the activation of NF-κB activities via distinct kinases and IκB proteins (9). The canonical pathway is induced largely by IκB kinase β (IKKβ), and targets the three canonical IκB proteins IκBα, IκBβ, IκBε. The non-canonical pathway is activated through IKKα, and utilizes the p52 precursor protein p100 (10), whose C-terminal ARD domains can function like an IκB protein to sequester NF-κB dimers in an active state (2). A third possibility is the IKK-independent "atypical" pathway of NF- κB induction, which is activated for example by DNA damages (5).

Remarkably, all IκB genes have been reported to be NF-κB target genes, providing a potential negative feedback loop (2). In recognition that these dynamic molecular interactions are critical for NF-κB signalling, the network of IKK, IκB and NF-κB proteins has been termed the NF-κB signalling mechanism (11). Indeed, NF-κB activation dynamics may be stimulus-specific (12) and can be regulated by critical mechanisms for the activation of stimulus-specific gene expression programs (2).

1.1.4 Regulation of the NF-κB transcriptional activity

As a central regulator of the transcriptional control of inflammatory genes, NF-κB function is not a steady-state or equilibrium phenomenon, but occurs in the context of highly dynamic signalling events. Indeed, the transient nature of gene expression is the basis for the resolution of inflammation. Molecular attenuation mechanisms that limit inflammatory signalling have therefore received great attention (13). Furthermore, NF-κB activities appear in the nucleus and on target genes with characteristic temporal profiles (2). Within this context, it is notable that NF-κB target genes show distinct temporal expression profiles (14).

Transcriptional control involves the coordinated function of many proteins, including DNA-bound transcription factors, co-activators and co-repressors in the context of nucleosomal chromatin. The formation of hetero- and homodimers of the five family members that are selectively regulated by IκB proteins is a primary source of transcriptional specificity. Specificity in transcriptional responses can, in part, be additionally provided through the combinatorial effects of transcription factors. However, there are additional factors that determine what constitutes an NF-κB-regulated gene for a given stimulus (2). Given the large number of proteins located in DNA regulatory sequences, protein-protein interactions are likely as important as transcription factor-DNA interactions in determining transcriptional specificity (2).

1.1.5 Induction of the NF-κB pathway by LPS

Primary human macrophages are sentinels of the immune system. Following infection, circulating monocytes migrate from the peripheral blood to tissues where they differentiate into resident tissue macrophages. Recognition of pathogen associated molecular patterns (PAMPS), including gram negative bacterial LPS, results in activation of macrophages, leading to a plethora of biological responses required for shaping both the innate and adaptive arms of the immune response (4). These effects are mediated through the release of chemokines and cytokines such as tumour necrosis factor α (TNFα) and interleukin 1b (IL-1b). However, excess release of these mediators can result in septic shock, multiple organ failure and acute respiratory distress syndrome (4).

When LPSs are present in the bloodstream, they are immediately captured by LPS-binding protein and then transferred to their cognate cellular receptor complex composed of CD-14, MD-2, and toll-like receptor 4 (TLR-4) (15, 16). Binding of LPS to the CD-14/MD-

2/TLR-4 receptor complex activates via TLR-4-associated MYD88 complexes a diverse set of signalling cascades including the TRAF6/TAK1/IKK-α/IKK-β-IκB-NF-κB pathway. In macrophages, NF-κB might subsequently upregulate in concert with different other co-activators (e.g. PARP1) the expression of specific sets of pro-inflammatory mediators involved in the pathogenesis of inflammation such as cytokines (TNFα, MIF, IFN-γ) or interleukins (IL-1b, IL-6, and IL-8). The massive production and release of cytokines by macrophages might then in turn activate leucocytes and other inflammatory cells (1).

1.2 Poly(ADP-ribose) polymerase 1

1.2.1 Introduction

Mammalian poly(ADP-ribose) polymerase 1 (PARP1) is an abundant nuclear chromatin-associated protein. PARP1 catalyzes the transfer of ADP-ribose units from its substrate β-nicotinamide adenine dinucleotide (NAD+) covalently to itself and other nuclear proteins (1). PARP1 was identified by Pierre Chambon et al. in 1963 (17). Ubiquitous PARP activity has been found in organisms ranging from archaebacteria to mammals, although it is apparently absent in yeast (1). PARP1, a 113 kDa protein, is the prototypical and most abundantly expressed member of the PARP family (18).

1.2.2 The PARP family

For a long time, the best-investigated PARP protein, PARP1, has been thought to be the only enzyme with poly(ADP-ribosyl)ation activity in mammalian cells. However, this view has been challenged by the development of mice deficient in PARP1 (19). Primary cells derived from PARP1 knockout (-/-) mice could still synthesize poly-ADP-ribose following treatment with DNA-damaging agents (20). The “PARP signature” from the catalytic domain (see 1.2.3) was used to search non-redundant protein databases from the National Center for Biotechnology Information (NCBI) for human PARP homologues. Subsequently, five new genes encoding “bona fida” PARP enzymes have been identified (21), indicating that PARP1 belongs to a family of poly(ADP-ribose) polymerases (22). Later, additional putative PARPs were identified, which increased the number of PARP-family members to 17. It has however to be confirmed whether these proteins are “real” poly(ADP-ribose) polymerases or whether they have only mono(ADP-ribosyl) transferase activity (23). Noteworthy is PARP2, which

seems to be most closely related to PARP1 in terms of structure and function (21). Both proteins are nuclear proteins and were reported to play important roles in the cellular response toward stress (24). The functions of the other PARP family members appear to be quite diverse, but are less well characterized.

1.2.3 Structure of PARP1

The structure of PARP1 has been extensively characterized (25). PARP1 is a highly conserved multifunctional enzyme consisting of three domains: a DNA-binding domain (DBD) containing a bipartite nuclear localization signal (NLS), which is interrupted by a caspase cleavage site, an automodification domain and a catalytic domain. The catalytic domain is the most highly conserved region of PARP 1 (25, 26), (Fig. 2).

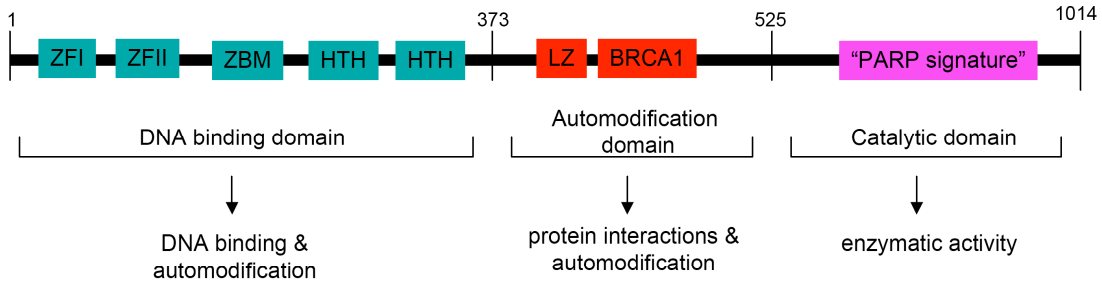

Figure 2: Structure of PARP1.

The N-terminal DBD of human PARP1 spans residues 1-373 and has a molecular mass of approximately 42kD. This domain contains two zinc fingers, the zinc binding motif and two helix-turn-helix (HTH) motifs. The two zinc fingers act as a "nick sensor" and recognise DNA damage. Two studies have shown that the zinc fingers are the main structures responsible for binding to double-strand breaks (DSBs) or single-strand breaks (SSBs) and for the activation of PARP1's enzymatic activity (27, 28).

The automodification domain of human PARP1 extends from residues 374 to 525 bearing a leucin zipper (LZ) motif in the N-terminal part and a BRCA1 carboxyl-terminal protein interaction domain (BRCT) from residues 384 to 479 in the C-terminal part. Both the LZs and the BRCT domain are well known to be involved in protein-protein interactions (1). The two zinc fingers, as well as the auto modification domain are both modified covalently by poly(ADP-ribose) (PAR).

The catalytic domain of PARP1 is located in the C-terminal part of the enzyme between residues 526-1014. The C-terminal domain (residues 795 to 1014) of the catalytic domain shares several structural features with other mono(ADP-ribosyl) transferases including an evolutionarily conserved region, called the “PARP signature”, spanning residues 859-908 (1).

1.2.4 Enzymatic activity of PARP1

Poly(ADP-ribose) is a homopolymer of ADP-ribose units linked by glycosidic bonds and synthesized by members of the PARP family (1, 24, 25). Comparable to mono-ADP-ribose synthesis, poly(ADP-ribose) (PAR) synthesis requires NAD+ as a substrate. The constitutive levels of poly(ADP-ribose) are usually very low in unstimulated cells (25, 29). However in response to mitogenic stimuli or genotoxic stress, the PARP activity and the levels of poly(ADP-ribose) may increase 10 to 500-fold, while cellular NAD+ levels are correspondingly reduced (22).

1.2.4.1 Poly-ADP-ribosylation reaction

ADP-ribosylation reactions play important roles in many physiological and pathophysiological processes, including DNA repair, cell cycle, necrosis, apoptosis and transcription. PARP1’s catalytic domain supports multiple distinct reactions that lead to the synthesis of PAR: (i) initiation (auto-mono(ADP-ribosyl)ation), (ii) elongation, and (iii) branching (30). PAR exists as free (non protein bound) or protein-associated polymers, which are covalently or non-covalently bound to proteins (Fig. 3). The exact acceptor sites of PAR in proteins or in PARP1 itself are not yet known.

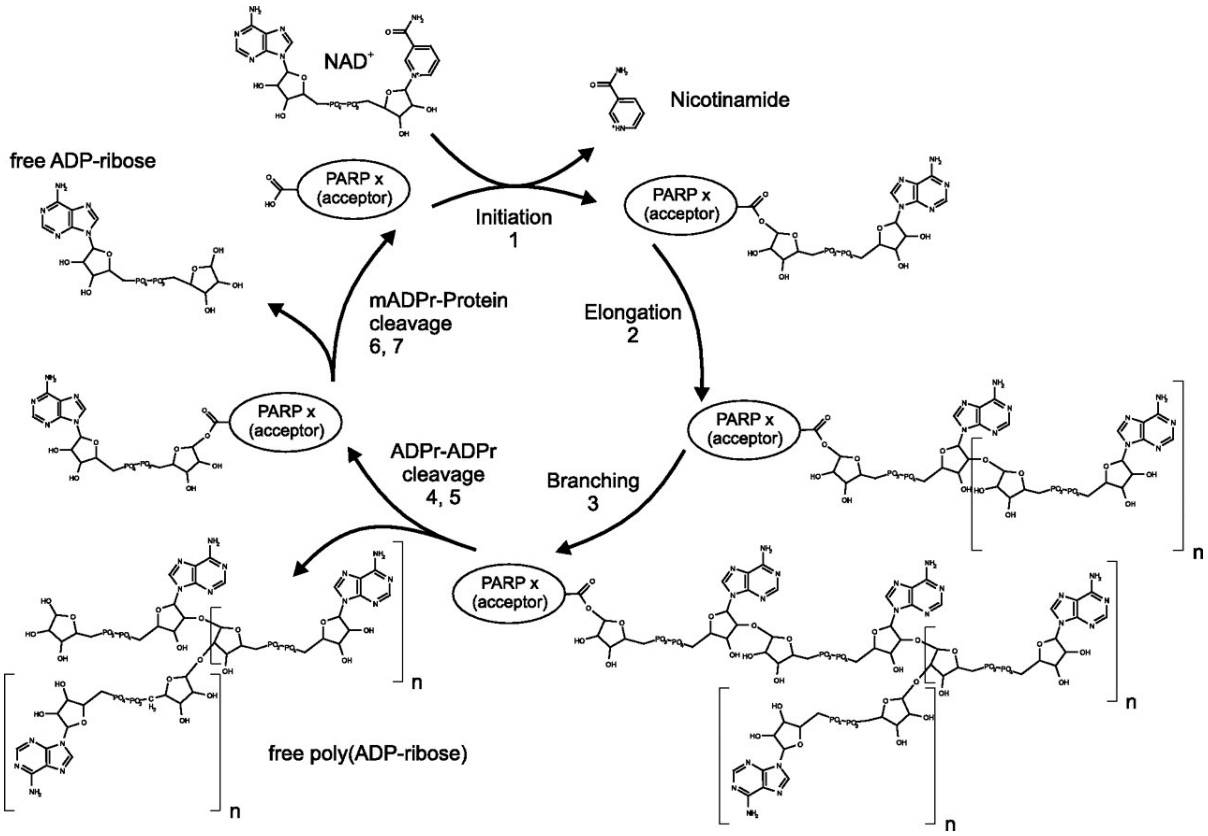

Figure 3: Poly(ADP-ribose) metabolism. Steps 1 to 3 and 4 to 7 represent the anabolic and catabolic reactions, respectively, in the metabolism of poly(ADP-ribose). The synthesis of poly(ADP-ribose) consists of three distinct PARP activities: 1) initiation of mono-ADP- ribosylation of specific residues in the acceptor chain, 2) elongation of the polymer, 3) branching of the polymer. Figure adapted from (22).

1.2.4.2 Structure of poly(ADP-ribose)

The chemical structure of poly(ADP-ribose) is well characterized. The ADP-ribose units in the polymer are linked by glycosidic ribose-ribose 1'-2' bonds. The chain length of polymers is heterogenous and can reach 200 to 400 units *in vitro* and *in vivo* (22, 31). Long polymers are branched in an irregular manner. Branching occurs *in vitro* and *in vivo* with a frequency of approximately one branch per linear section of 20 to 50 units of ADP-ribose (31, 32). PAR was postulated to bind to specific acceptor sites, which are unfortunately not yet indentified.

1.2.4.3 Catabolism of poly(ADP-ribose)

The breakdown of free (non-protein-bound) or protein-bound linear or branched PAR is mediated by poly(ADP-ribose) glycohydrolase (PARG), an enzyme with both exo- and endoglycosidase activities that hydrolyses the glycosidic bond between ADP-ribose units, and thereby generates free ADP-ribose (23) (Fig. 3).

1.2.5 Cellular functions of PARP1

PARP1 was reported to play a crucial role in many physiological and pathophysiological processes including inter- and intracellular signalling, cell cycle regulation, DNA replication, DNA repair, V(D)J recombination as well as regulation of telomere length (1, 22). Other functions proposed for PARP1 include transcription and gene expression, chromatin organization, proliferation and differentiation, cellular NAD+ metabolism, and mitosis, as well as necrosis and apoptosis (1, 22).

1.2.5.1 Role of PARP1 in transcription

The regulation of gene expression requires a wide array of protein factors that can modulate chromatin structure, act at enhancers, function as transcriptional coregulators, or regulate insulator functions (22). Biochemical, genomic, proteomic, and cell-based studies have highlighted the role of PARP1 in each of these processes and provided new insights about the molecular mechanisms governing PARP1-dependent regulation of gene expression (22).

Two different models were described for the interactions between PARP1 and the transcription machinery. The first model does not require the enzymatic activity of PARP1 and describes the direct binding of PARP1 to transcription factors including NF-κB (1, 33, 34) and thus influences the transcription machinery as “classical” transcriptional regulator or co-regulator (18, 25, 35) (Fig. 4A). The second model focuses on the remodelling of the chromatin structure which requires high enzymatic activity of PARP1 and poly(ADP)ribosylation of the histone proteins (Fig. 4B).

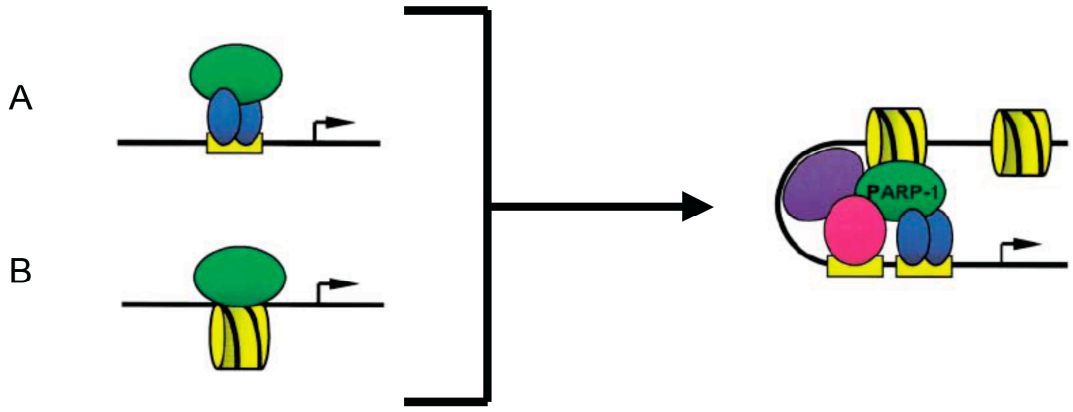

Figure 4: Two models for the involvement of PARP1 in transcription. Model A: PARP1 at enhancer and promoter regions and binding to transcription factors. Model B: PARP1 modulated the chromatin structure. Figure adopted from (18).

1.2.5.2 Role of PARP1 in DNA repair

PARP1's enzymatic activity correlates with DNA damage. PARP1 detects DNA nicks very efficiently with its two zinc fingers. The enzymatic activity of PARP1 has been shown to be strongly stimulated by the presence of DNA damage (18, 36). The observed affinity of histones to poly(ADP-ribose), especially attached to PARPs, led to the proposal of the 'histone shuttle' mechanism for chromatin relaxation and recondensation in response to DNA damage (36-38).

After activation by DNA strand breaks at the site of damage, PAR synthesized by PARP1 and to lesser extent by PARP2 would serve as a scaffold onto which histones could be sequestered thus dissociating from DNA in order to render DNA accessible to the repair machinery, facilitating repair of damaged DNA (25, 36, 38, 39).

Alternatively, histones as main protein component of the chromatin, might be directly modified by PARPs, which would lead to their dissociation from the DNA. Histones H1 and H2B were shown to be poly(ADP-ribosyl)ated *in vivo* and to be the preferred targets of PARP1 *in vitro* (40, 41). The resulting PAR production would also signal to the cells that the DNA was damaged and to which extent, thereby allowing the cell to establish an appropriate and adaptive response according to the severity of the injury (DNA repair or cell suicide, see 1.2.5.3).

1.2.5.3 Role of PARP1 in cell death

PARP1 was found to influence both necrosis and apoptosis (22). A striking model which would explain the observed phenotype for necrosis is the link between NAD+ consumption by PARP1 and ATP turnover (42). The model hypothesizes that upon overactivation of PARP1, PARP1 plays the role of a suicide molecule by depleting the NAD+ and ATP pool, thereby inducing cellular dysfunction and finally necrosis (43, 44). Since apoptosis is ATP-dependent, PARP1 can be seen as a switch molecule that shuts down apoptosis and promotes necrosis.

Other studies however provide evidence that PARP1 can also be a positive regulator of apoptosis. Shuttling of apoptosis-inducing-factor (AIF) from the mitochondria to the nucleus is a hallmark of apoptosis (45). When cells were treated with a PARP inhibitor, shuttling of AIF was attenuated in a mouse model of heart failure (46). The same AIF shuttling was attenuated in PARP1(-/-) cells, which were subjected to oxidative stress, indicating that PARP1 might be involved in promoting apoptosis. It is however not yet clear

how the signal by PARP1 is transduced from the nucleus to the mitochondria and whether it is PARP1 itself or its polymers which act as signals (47). Interestingly, PARP1 is cleaved into a 24 kDa N-terminal and a 89 kDa C-terminal fragment by caspases during apoptosis, which abrogates its enzymatic activity (48). However, this cleavage of PARP1 is rather a consequence of the apoptotic program than a required event, since mice with non-cleavable PARP1 showed no defect in apoptosis (49). According to the "double-edged sword" role, PARP1 was suggested to activate upon mild to moderate genotoxic stimuli first DNA repair. As a consequence DNA damage would be repaired. Upon more severe DNA damages, PARP1 would induce cell death. This pathway allows cells with unrepairable DNA damage to become eliminated in a safe way. Cleavage of PARP would avoid hyperactivation of PARP1 by the ensuing DNA fragmentation, thus preventing cells from the pathological sequelae of necrosis, a less controlled mechanism posing danger for bystander cells (50).

1.2.6 Mouse model

To study PARP1 *in vivo*, several PARP1 knockout (-/-) mouse models have been developed (51, 52). Noteworthy, only a part of the suggested functions of PARP1 based on *in vitro* results could be confirmed *in vivo*. PARP1 -/- mice are viable and fertile, but were reported to be protected against various disease models (53). A pathophysiological role of PARP1 has been demonstrated in a number of diseases and animal models, including streptotocin-induced diabetes (54-56), zymason-induced vascular failure, a non-septic model of multiple organ dysfunction (57), LPS-induced septic shock, and carrageenan-induced pleurisy (58, 59), as well as collagen-induced arthritis (CIA), a model for chronic inflammation (60). Cerebral ischemia is characterized by insufficient blood flow in the brain. It causes brain damage and death depending on the duration and severity of the condition. PARP1(-/-) mice were reported to be protected against cerebral ischemia (53). Interestingly, PARP1 enzymatic activity was strongly activated during this process. Consequently, PARP1 inhibitors were suggested as therapeutics in the treatment of cerebrovascular diseases (61). The bacterial endotoxin lipopolysaccharide (LPS) activates inflammation through toll like receptors and causes septic shock in individuals exposed to large LPS doses. When PARP1(-/-) mice were treated with high doses of LPS, all of them survived while most of their wild type littermates died (58, 62). Studies with mice lacking either PARP1 or PARP2 provide evidence for protection against cell death in disease models (53, 63).

An attempt to create PARP1(-/-)/ PARP2(-/-) double knockout mice failed. Mice died during embryonic development, suggesting that PARP1 and PARP2 are involved in the same functions (64).

The proposed role of PARP1 as DNA damage sensor suggests that PARP1 works in concert with DNA repair proteins to protect the organism against mutation and transformation which would therefore be beneficial to prevent cancer. Indeed, PARP1(-/-) mice demonstrated increased carcinogenesis after treatment with alkylating agents (65). The double knockout mouse PARP1(-/-)/ p53(-/-) spontaneously develops brain tumor, further supporting the protective role of PARP1 in cancer (66). On the other hand, another group using a different strain of PARP1 (-/-)/ p53 (-/-) mice, reported attenuated tumor formation compared to wild type mice (67). The above mentioned contradiction could be explained by differences between various types of cancers and the fact that cancer is a complex, multi-step phenomenon on which PARP1 could have an influence via several mechanisms.

Along the same line, treatment of mice with PARP inhibitor suppressed tumorgenesis in a TPA-induced skin cancer model (68), suggesting an imported role for the enzymatic activity of PARP1. One possible explanation for this positive effect of PARP inhibitors on carcinogenesis is the reported oncogenic potential of iNOS in a p53(-/-) background, a gene which is regulated by PARP1 (see below).

1.2.7 The role of PARP1 in LPS induced septic shock

The regulation of immune and inflammatory response is a complex physiological process that is of profound importance to both homeostasis and ultimate survival of an organism. Without inflammation and activation of the immune system, an organism could not survive the insult of injury or would rapidly succumb to invading pathogens (1). The inflammatory response is composed of an elaborate cascade of inflammatory mediators. Their regulation must be tightly coordinated to maintain appropriate and timely immune reactions without an over-reaction that can cause damage to the host. Yet, without mechanisms that shut down prolonged, inappropriate, or excessive immune response and inflammation, the organism would die from damage caused by these physiological responses. Therefore, both pro- and anti-inflammatory mechanisms must be activated and balanced for an organism to survive in the face of environmental stimuli that elicit an immune response (1).

Septic shock is the most common cause of death in intensive care units, with a high mortality rate, often as a result of a systemic gram-negative bacterial infection (1). It is

defined as an acute circulatory failure or dysfunction of a number of organ systems associated with severe sepsis, persisting despite adequate fluid resuscitation, causing a shock-like state and leading to death (69, 70). Septic shock can be mimicked in animals by intravenous injection of microbial products such as bacterial LPS (71). LPS activate a complex signalling cascade, enabling the expression of many crucial genes involved in the pathogenesis of septic shock, such as cytokines (e.g., TNF-α, IL-1b,) (69, 72). One of the striking features of septic shock is the increased production of peroxynitrite which can induce massive levels of DNA SSB and activation of the PARP1 "suicide-pathway", resulting in necrotic cell death and endothelial dysfunction (73). It was showed that PARP inhibitors can strongly reduce tissue damage caused by high doses of endotoxin (73). Moreover, recent studies from different groups reported that PARP1(-/-) mice were extremely resistant to LPS-induced lethality (58, 62). The production of peroxynitrite and neutrophil recruitment during endotoxic shock as well as local and systemic inflammation were drastically reduced in the absence of PARP1 (58, 62).

1.2.8 PARP1 as co-activator of NF-κB

There are striking similarities between the expression pattern of PARP1 and the detrimental transcriptional activity of NF-κB. In most tissues and cell types associated with high PARP1 expression, dysregulated NF-κB activity seems to contribute to cellular dysfunction and necrotic cell death during inflammatory disorders (1). The relative contribution of NF-κB transcriptional activity to either a "good" inflammation, manifested by cell survival and tissue regeneration, or a "bad" inflammation, causing dell death and tissue destruction, rather depends on the kinetics of activation and intrinsic metabolic differences between different cell types or within the same cell and on the natures as well as intensity of the activating stimulus (1, 74, 75).

Several reports showed that PARP1 is required for specific NF-κB-dependent gene activation and can act as a coactivator for NF-κB *in vivo* (35, 58, 76). PARP1 was shown to be required and sufficient for specific transcriptional activation of NF-κB in response to pro-inflammatory stimuli and genotoxic stress. Neither the nuclear translocation nor the DNA-binding ability of NF-κB were affected in PARP1(-/-) cells (1, 35, 58, 76). However, PARP1 directly interacted through different domains with both subunits of NF-κB (p65 and p50) *in vitro* and formed a stable immunoprecipitable nuclear complex together with p50 and p65 *in vivo*, which was independent of DNA (1, 35, 76). Surprisingly, neither the enzymatic activity

of PARP1 nor its DNA-binding activity was required for full activation of NF-κB in response to various stimuli *in vivo* (76, 77). The strongest indication for a direct role of PARP1 in NF-κB-dependent transcription is the impaired expression of NF-κB-dependent pro inflammatory mediators in PARP1(-/-) mice (53). The fact that PARP1(-/-) mice do not show the same phenotype compared to RelA/p65(-/-) animals, indicates that only subsets of NF-κB-dependent genes are dependent on PARP1, such as iNOS or TNF-α. RelA/p65 was described to interact directly with the basal transcription machinery as well as with distinct sets of transcriptional co-factors and co-activators (1, 78). Thus, in certain instances, the requirement for PARP1 is possibly bypassed through other specific co-activators and co-factors, most probably in a cell type- and stimuli-dependent manner (1).

1.3 Cell cycle

1.3.1 Introduction

The cell cycle, or cell division cycle, is the series of events that take place in a eukaryotic cell leading to its duplication (79, 80), (Fig. 5). These events can be divided in two brief periods: Interphase and mitotic phase.

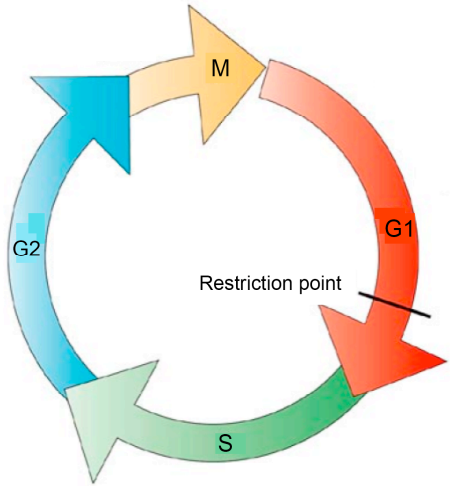

Figure 5: Cell cycle phases. G1 = growth phase 1, S = synthesis of DNA, G2 = growth phase 2, M = mitosis (80).

During the mitotic phase the cell divides into two daughter cells. During the rest of the cycle (the Interphase) the cell is constantly synthesizing RNA, producing protein, growing in size and duplicating its DNA (79). Interphase generally lasts at least 12 to 24 hours in

mammalian tissue. Mitosis is much shorter than interphase, lasting only one to three hours (79).

1.3.2 Cell cycle phases

Throughout interphase, the cell is engaged in growth and metabolic activities. Interphase can be further broken down into 3 discrete phases named G1, S and G2. During G1 or first growth phase, cells grow and prepare for the replication of their DNA. In S phase, synthesis of DNA takes place by producing two DNA replicates of each chromosome. During G2 phase, the cell continues to prepare for mitosis and cell division (79).

Mitosis or the mitotic phase has four stages: Prophase, metaphase, anaphase and telophase (79). During prophase the chromosomes become visible and condense, shorter and thicker. Each identical copy of a single chromosome is called a sister chromatid. The nuclear envelope breaks down and spindle fibers form as microtubules grow out of the centrioles that move to opposite poles of the cell. During metaphase, the chromosomes line up along the equator of the cell. The spindle is now fully formed and the microtubules attach to each sister chromatid. Anaphase begins when the sister chromatids of each chromosome begin to separate. The centromere that holds sister chromatids together divides and the chromosomes move away from each other along the spindle fiber. In telophase, the two groups of chromosomes reach the opposite ends of the cell. As a result of the previous nuclear envelop break down, two new membranes starts to form around each group, the chromosomes uncoil and the spindle disappears. The division of the cytoplasm and organelles is called cytokinesis. The result of mitosis and cytokinesis is the formation of two genetically identical daughter cells (79).

1.3.3 Control of the cell cycle

Regulation of the cell cycle involves crucial steps, including detection and repair of genetic damage. The progression through the cell cycle is controlled by proteins. Two key classes of regulatory molecules, cyclines and cyclin-dependent kinases (CDKs) are responsible for this regulation (81). The protein levels of cyclines (cyclin D (G1 phase), cyclines E and A (S phase), and cyclines B and A (mitotic phase)) rise and fall with the stages of the cell cycle, while the protein levels of CDKs (CDK4 (G1), CDK2 (S phase), and CDK1 (mitotic phase)) remain fairly stable (Fig. 6).

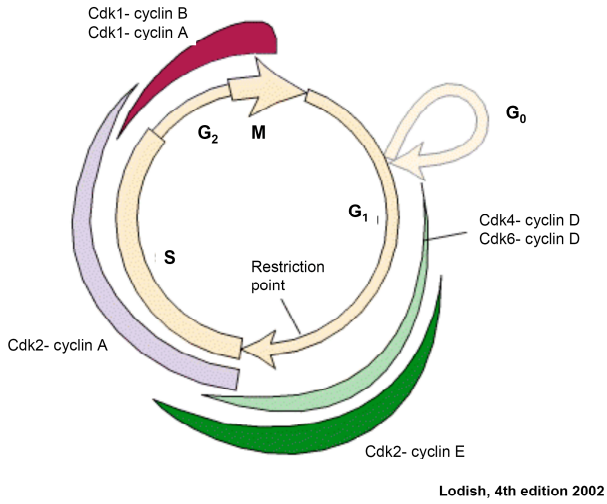

Figure 6: Cell cycle phases and corresponding Cdk-Cyclin levels (79).

Each CDK must bind to its appropriate cyclin (whose levels fluctuate) in order to be activated. The availability and formation of the cyclin-CDK complex thus allows progression through the cell cycle (81).

1.3.4 Cell cycle synchronization

Cell synchronization is required to study the behaviour of the cells in different cell cycle stages. Synchronization is achieved by two different techniques – physical cell separation and chemical blockade (82). Physical cell separation is performed based on cell density, cell size, affinity of antibodies and on fluorescent emission by labelled cells. Cell synchronization by chemical blockade can be caused by nutritional deprivation or by chemicals interfering with DNA synthesis or by inhibiting microtubules dynamic. DNA synthesis inhibitors are used to arrest the replicating cells in S phase. Inhibitors commonly used are those that inhibit the synthesis of deoxyribonucleotide triphosphates, such as thymidine at high concentrations or more drastically hydroxyurea. Alternativly the direct DNA polymerase inhibitor aphidicolin can be used.

To arrest cells at G2/M phase the antimitotic agent nocodazol is often used. It disrupts microtubule formation by binding to β-tubulin and prevents formation of one of the two interchain disulfides linkages. Nocodazol disrupts subsequently the mitotic spindle function, and induces fragmentation of the golgi complex. As a result, cells are arrested in G2/M phase (83). Usually, cells that are not in the preferred phase at the time of treatment with inhibitors, will be arrested when they pass the phase the next time (82). Prolonged treatment with

thymidine, hydroxyurea and aphidicolin can be toxic to cells, and thus does not always block cells securely at the G1/S boundary (82).

One way to assess the phase of cells, is by measuring its DNA content, which doubles during S phase. This approach is greatly facilitated by the use of a DNA-binding fluorescent dye (PI) and the fluorescence activated cell sorting machine (FACS), which allows the rapid analysis of a large number of cells (84).

1.4 Connection between cell cycle and NF-κB or PARP1

1.4.1 Cell cycle and NF-κB-transcriptional activation

The transcriptional activity of a cell has to be tightly controlled during the cell cycle, since transcription and replication are both using DNA as template (79). During G1 and G2 phase only transcription takes place. The challenges for the transcription during S phase are two-folded; first the DNA synthesis induces the relaxation of the chromatin structure and thus allows transcription factors to bind more easily to the DNA. Second, ongoing replication might interfere with transcription at the same DNA strand (79). During mitosis the cell faces various additionally challenges, since chromatin condensation and numerous mitotic activities might interfere in different ways with the binding between the transcription factors and the chromatin (79).

Some investigation how NF-κB transcriptional activity is regulated during cell cycle has been recently reported (85). Perkins and co-workers showed that the processing of the p100 NF-κB subunit to p52 is inhibited in U2OS cells and MEFs during S phase. They also reported that RelA/p65 phosphorylation changes during cell cycle. RelA is predominantely phophorylated at S468 in G1 phase, while S536 phosphorylation is low in G1 phase but becomes apparent in S phase and is peaking in G2 phase. This differential RelA/p65 phosphorylation in the G1 and G2 phases is IKK-dependent (85). These observed mechanisms go along with parallel control of important target genes during cell cycle, what results in activated cyclin D1, c-Myc and Skp2 expression during G1 phase and reduced cyclin D1, c-Myc and Skp2 expression during S and G2 phase (85). Taken together, these data reveal a previously unknown and dynamic regulation of NF-κB activity across the cell cycle. Although many of these activities depend at some level on IKKα or β, observations suggest that other signalling pathways must coordinate these events and integrate with the

NF-κB signalling pathway in a cell cycle-dependent manner. It was also reported that active Akt and Chk1 fluctuate during cell cycle and regulate IKK/NF-κB activity (85).

1.4.2 Cell cycle and PARP1

Poly(ADP-ribosyl)ation plays an important role in a large variety of physiological processes also including cell cycle, but its role in cell cycle progression is not yet defined (50). Recently a functional interaction between mitogen-activated protein kinase (MAPK) signalling and PARP1 activation was reported (50). It has been well established that the MAPK pathway plays an important role in the activation of the cell cycle machinery in mitogen stimulated cells, thereby suggesting a possible role of PARP activity in linking growth factor signalling with cell cycle entry (50). Whether the enzymatic activity of PARP1 is dependent for the propagation through the cell cycle phases has not yet been investigated.

1.5 Aim of this thesis

Despite the notable physiological relevance of NF-κB, little details are known about the nuclear mechanism enabling NF-κB-dependent gene expression during the different phases of the cell cycle.

The aim of this thesis was to shed light on the physiological role of PARP1 as transcriptional co-factor for NF-κB-dependent gene expression during the cell cycle. A better understanding of the NF-κB physiology and of factors influencing the expression of NF-κB target genes is of great importance, since NF-κB has been implicated in different cellular processes and in a broad range of diseases, such as LPS induced septic shock.

2 Results

2.1 LPS induces NF-κB target genes in RAW 267.4 macrophages

In order to investigate the functional relevance of PARP1 in transcription, we stimulated RAW 267.4 macrophages with LPS (10 μg/ml for 1 hour). Total RNA was isolated and several genes were analysed by qRT-PCR. Chosen genes had already been described to be NF-κB target gene or were known to be important for the regulation of inflammation. Finally some genes were selected based on own previous observations (unpublished data), (Tab. 1).

Gene	Primer	Fold induction upon LPS stimulation
Icos	bad	n.d.
IL-1b	good	1000
IL-6	bad	n.d.
IL-12	good	400
IL-15	good	0
TNFα	good	50 - 400
IP-10	good	480
Cdyl2	bad	n.d.
Stat1	bad	n.d.
Mpa2l	good	0
Ccrl1	bad	n.d.
cd48	bad	n.d.
Hif1an	good	0
Tnc	bad	n.d.
Igfbp	bad	n.d.
Lif	good	85
Csf2	good	45
PARP2	good	0
PARP1	good	0
RPS12	good	0
GAPDH	good	0

Table 1: Table of all genes we investigated with our cell synchronization system. Bad = no specific product formed, good = single specific product was formed before cycle 35, 0 = no difference between stimulated versus unstimulated, n.d. = not detectable, due to non-functional primer (e.g. Primer dimmer formation or low detectable mRNA content.

While for some genes the RNA could not be detected by qRT-PCR, most probably due to inappropriate primers, other genes such as IL-1b, IL-12, IP-10, Csf2, Mpa2l or Lif could be quantified and showed a strong induction by LPS (Tab. 1). Gene expression was normalized to RPS12 or GAPDH, two genes that were earlier described not to be affected by LPS or the cell cycle. A third group of target genes was not stimulated by LPS (e.g. IL-15, Hif1an). We therefore decided to further analyse the following six LPS induced genes, in a more detailed manner: IL-1b, Csf2, IL-12, IP-10, Mpa2l and Lif.

2.2 Knockdown of PARP1 by a short hairpin RNA construct results in a stable reduction of PARP1 protein levels in RAW 267.4 macrophages

In order to investigate the possible involvement of PARP1 in NF-κB-dependent gene expression, a PARP1 knockout or knockdown cell system and the corresponding control cells are required. Therefore, PARP1 was knocked down in RAW 267.4 macrophages by a short hairpin (sh) RNA approach. Parental RAW 267.4 macrophages were transduced with a retrovirus constitutively expressing either a shPARP1 or a shMock (scrambled sequence) RNA construct. Upon transduction, cells were selected for successful integration. The efficiency of the shPARP1 construct to knockdown PARP1 was tested by Western blot analysis using an anti-PARP1 antibody. Western blot analysis revealed a distinct signal for cells expressing shMock and no signal of PARP1 for cells expressing the shPARP1 construct (Fig 7A), indicating that the knockdown was very efficient.

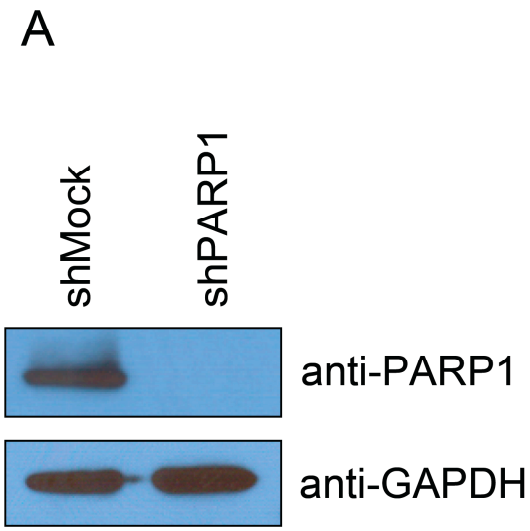

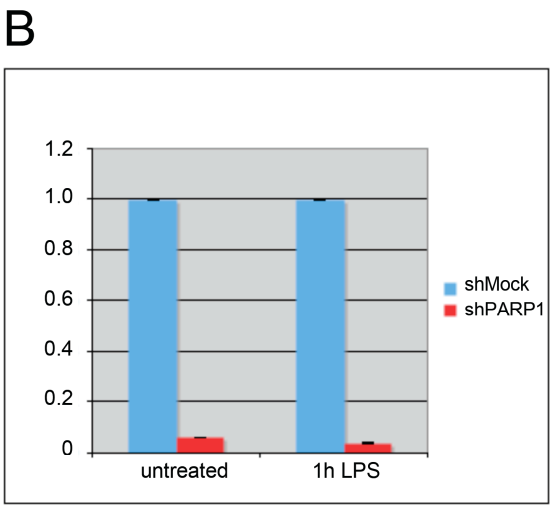

Residual PARP1 mRNA levels:

untreated	5.8%
1h LPS	3.7%

Figure 7: shPARP1 knockdown was controlled by Western blot (A) and qRT-PCR (B) for PARP1. For the qRT-PCR both unstimulated and 1h stimulated (LPS, 10µg/ml) shMock or shPARP1 cells were examinated.

Additionally, the absolute PARP1 gene expression levels in unstimulated or LPS stimulated shMock or shPARP1 cells were analysed by qRT-PCR. qRT-PCR results revealed that the PARP1 mRNA levels were drastically decreased in shPARP1 cells. The residual PARP1 mRNA levels were less than 6% or 4% for unstimulated or LPS stimulated cells respectively (Fig. 7B). LPS itself did not alter PARP1 expression.

These data confirmed that the retroviral shRNA successfully reduced PARP1 protein levels. Additionally, the shMock cells provide an appropriate control for the tested system.

2.3 PARP1 functions in unsynchronized cells dependent on the gene as transcriptional co-activator or as co-repressor

In order to define whether the six chosen genes were PARP1-dependent, shPARP1 and shMock cells were treated for 1 hour with LPS (10ug/ml). Total RNA was subsequently isolated and quantified by qRT-PCR (Fig. 8).

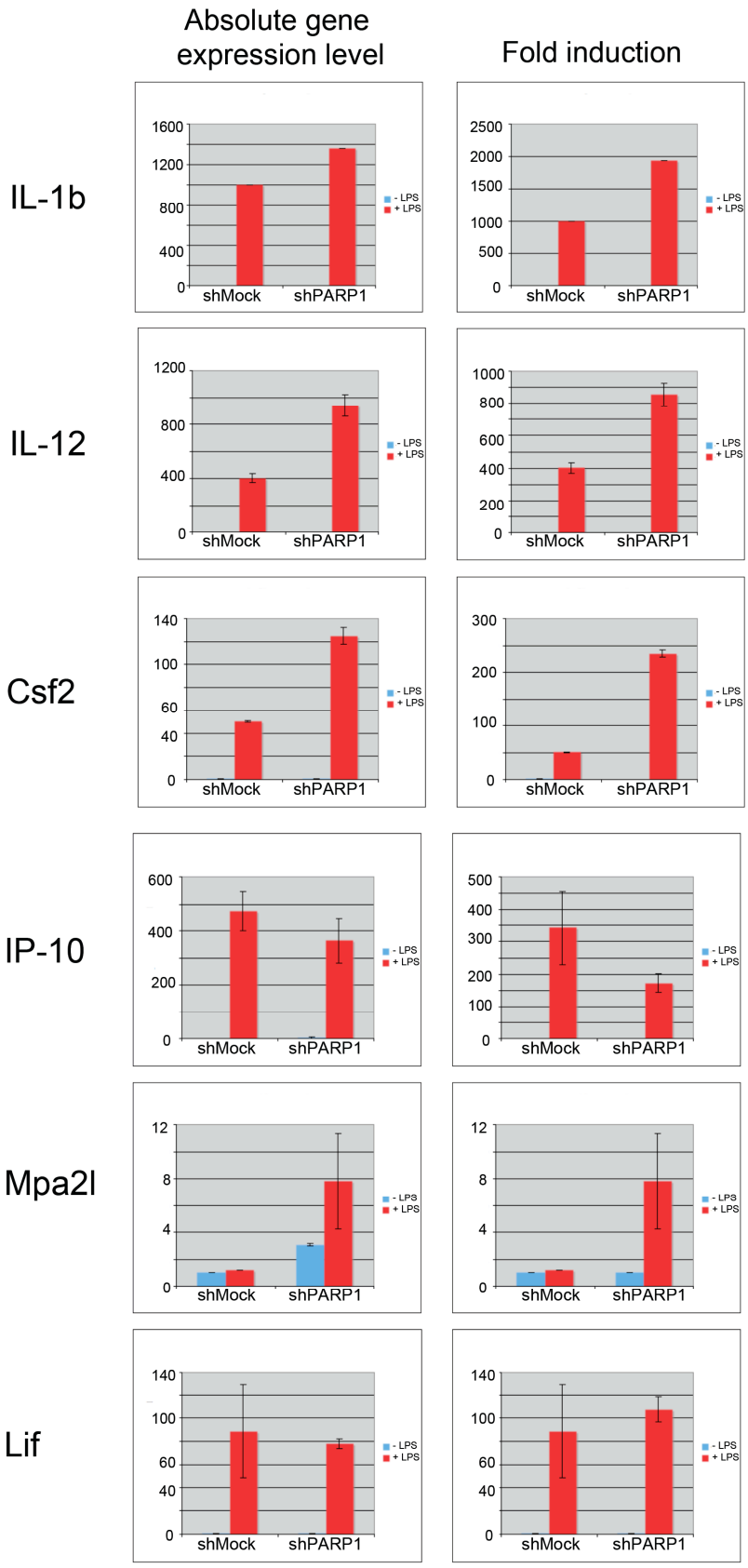

Figure 8: Unsynchronized shMock and shPARP1 RAW 267.4 macrophages were stimulated with LPS as indicated. RNA was isolated to analyse gene expression levels by qRT-PCR. The left panel shows the absolute gene expression levels from each gene (shMock unstimulated level set as 1) and the right panel shows the fold induction (unstimulated shMock and shPARP1 set as 1). Standard error bars are calculated from 2 or 3 biological replicates and additional 2 or 3 techniques replicates.

The quantification of the absolute mRNA gene expression levels of stimulated and unstimulated shMock or shPARP1 cells are shown in Fig. 8 left panel. shMock unstimulated value was arbitrary set to 1. In the same Figure (right panel), the fold induction is shown as the result of the stimulation difference between unstimulated and stimulated cells. Here both values from unstimulated shMock and shPARP1 cells were set to 1. Interestingly, while the expression levels of IL-1b, IL12, Csf2 and Mpa2l were reduced in shMock cells, suggesting that PARP1 functions as co-repressor, the expression pattern for IP-10 was exactly opposite (higher for shMock cells) suggesting that PARP1 acts for this gene as co-activator. Lif gene expression was not affected by the reduction of PARP1.

These data provide evidence that PARP1 acts dependent on the analysed gene either as transcriptional co-repressor or co-activator.

2.4 Induction of cell cycle arrests in shMock and shPARP1 RAW 267.4 macrophages

In order to investigate whether the cell cycle would effect NF-κB-dependent gene expression through the involvement of PARP1 as transcriptional co-factor, we synchronized the transduced cells by different chemical treatments. To arrest cells in the different cell cycle phases we treated them with either Thymidine, Aphidicolin or Nocodazol. Thymidine treatment causes a cell cycle block at the G1/S boundary (82). Upon treatment with Aphidicolin the cells should peak in early S phase, since Aphidicolin inhibits DNA polymerase (82). Nocodazol on the other hand inhibits microtubule dynamics, disruption of mitotic spindle function, and fragmentation of the golgi complex which results in a cell cycle arrest in G2/M phase (83). Cells were synchronized during 14 to 15 hours with the corresponding compound, subsequently treated with LPS for one hour to induce NF-κB. After this treatment of synchronization, stimulated or unstimulated cells were stained with Propidium Iodid (PI) to be able to analyse their cell cycle distribution by FACS.

The FACS analysis represents the fluorescence intensity, which correlates with the contents of DNA and the number of cells with the corresonding amount of DNA (fluorescence). Unsynchronized cells characteristically are distributed in two peaks. The first peak represents cells in G1 with a diploide genome (2n, 2c). The second peak represents cells with a replicated genome (2n, 4c) and correlates with cells in G2/M phase. Cells in between these peaks are in S phase, replicating the DNA content from 2c to 4c (Fig 9. top left panel).

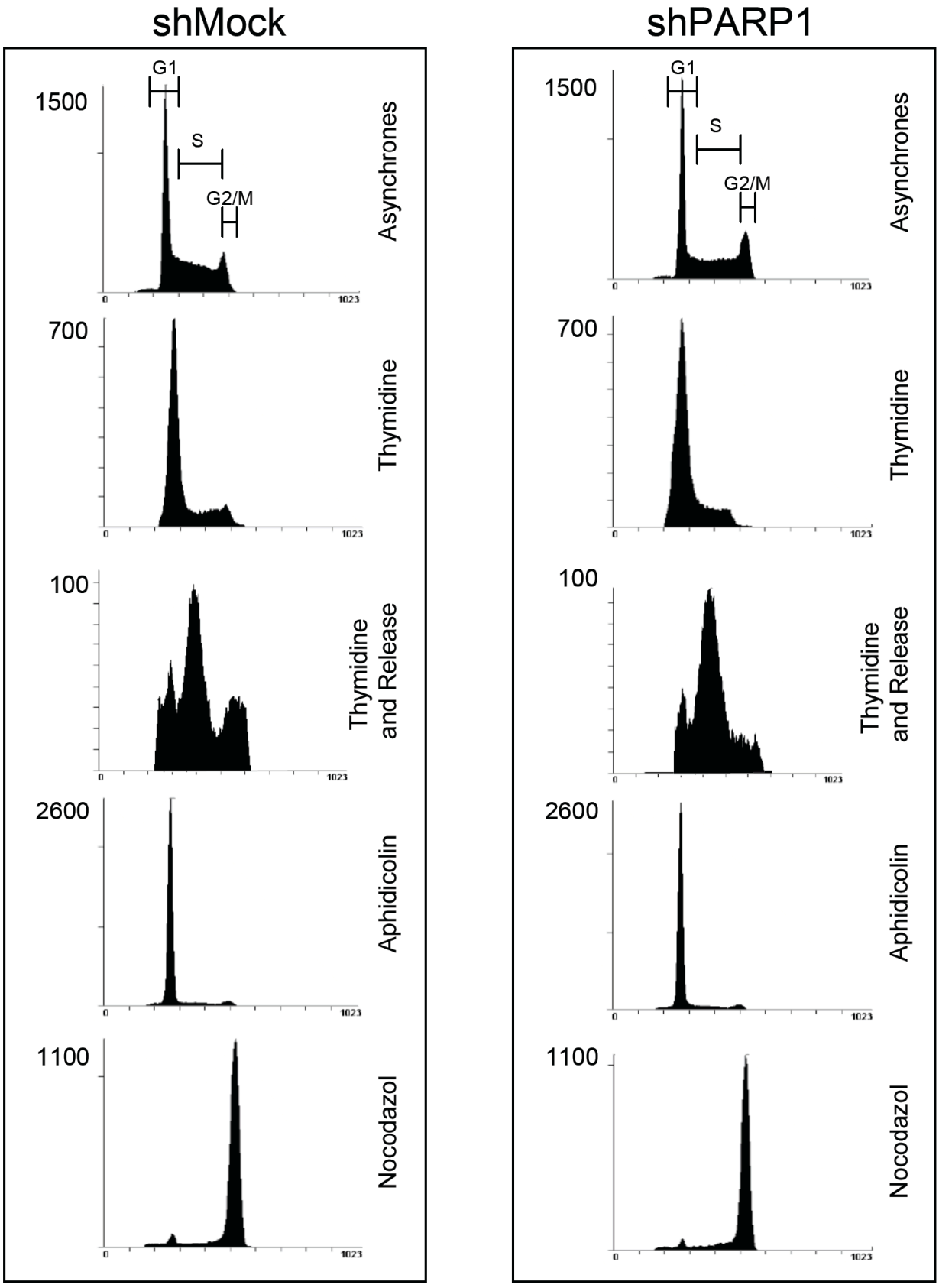

Figure 9: Unsynchronized cells were synchronized with the corresponding compound (Thymidine: 0.6 mg/ml, 15h; Aphidicolin: 5µg/ml, 14h; Nocodazol: 0.4µg/ml, 15h). Cells were PI stained and analysed by FACS, where always 10^3 cells were measured.

Treatment of cells with Thymidine arrested them to 73% in G1 (Fig. 9 and Tab. 2). After 3 hours release, the peak (representing 69% of the cells) moved to the right into S phase. Aphidicolin treatment also induced a nice G1/S peak. Noteworthy, this peak was very high on the y scale (up to 2600) and cells were synchronized very well (82%). After Nocodazol treatment the cells peaked in G2/M (83%).

Together, treatment of the cells with different compounds nicely arrested them in the corresponding phase of the cell cycle. Overall the treatment did not induce strong apoptosis, since not more than 8% of the cells died according to the FACS analysis. Additional treatment with LPS for 1 hour did not affect the cell cycle arrest (data not shown). Interestingly, lack of PARP1 did not affect cell cycle distribution (Fig. 9 right panel).

Synchronization treatment		% G1	% S	% G2/M	% dead cells
Asynchronous	shMock	50	34	13	2
	shPARP1	45	29	19	3
Thymidine	shMock	73	18	5	4
	shPARP1	72	16	4	5
Aphidicolin	shMock	83	8	4	4
	shPARP1	81	9	5	3
Thymidine +3h release	shMock	16	68	8	5
	shPARP1	18	69	4	6
Nocodazol	shMock	3	7	83	6
	shPARP1	3	8	81	7

Table 2: During FACS analysis the percentage of cells in each cell cycle phase was calculated by the machine. Numbers are from a representative experiment.

From these data we concluded: i) treatments synchronized cells at the expected cell cycle phase, indicating that the cellular cell cycle arrest mechanisms were intact in the analysed cells, ii) the established protocols are not too stressfully for the cells, since the amount of dead cells never exceeded 8%, iii) compounds synchronized the cells in a PARP1 independent manner (shMock vs. shPARP1) and independent of the stimulation by LPS.

2.5 Cell cycle synchronization induces poly(ADP-ribose) polymer formation

To test, whether the treatment with different cell synchronization compounds would affect the physiological function of PARP1, whole cell extracts were generated from the shMock RAW macrophages after each synchronization treatment. Extracts were subsequently analysed by Western Blot analysis using antibody against PARP1 or PAR. While PARP1 protein levels were not changed upon cell cycle synchronization, some treatments induced detectable PAR formation (Fig. 10 A and B).

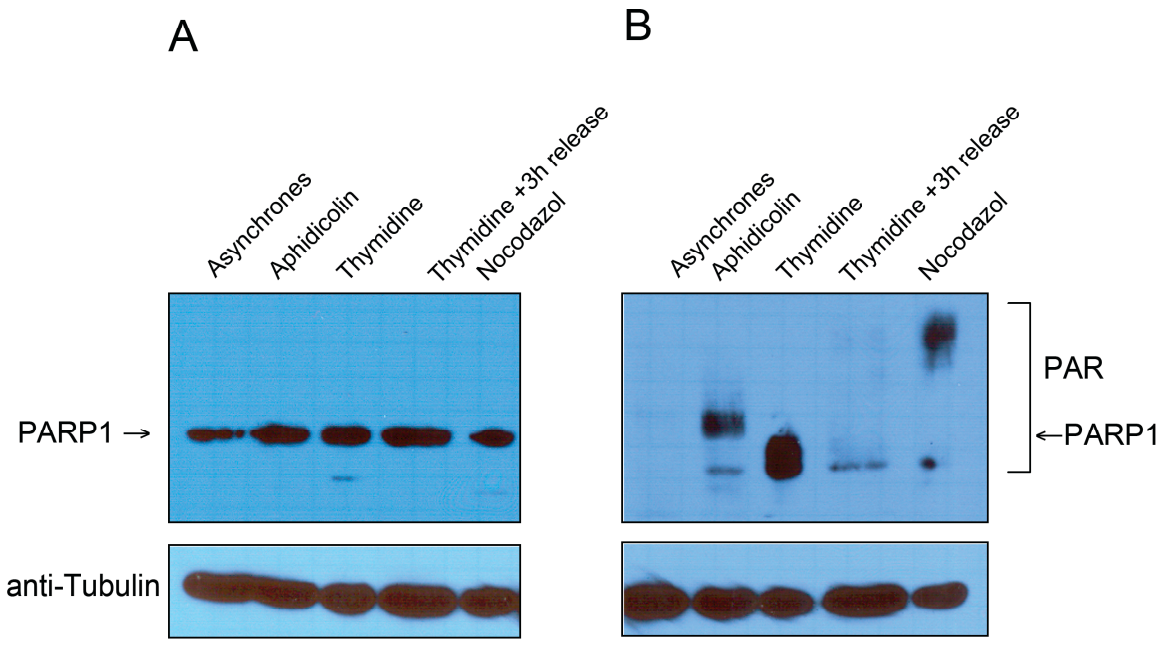

Figure 10: Whole cell extracts from shMock cells were isolated after each cell cycle block, and analysed by Western Blot. A: Western Blot using an anti PARP1 antibody. B: Western Blot using an anti PAR antibody.

Although Western Blot analysis does not allow a quantitative statement, it was obvious that the different treatment would induce PAR polymers of different quality and quantity. Aphidicolin and Thymidine induced rather short polymers and Nocodazol very long one. Release of cells from Thymidine block resulted in a much weaker PAR signal, suggesting that formed PAR was subsequently degraded again. Interestingly the PAR induction did not induce strong apoptosis (see above) under the tested conditions.

Together these results suggested, that synchronization of cells with chemical compounds is inducing PARP1's enzymatic activity and might influence the function of PARP1 and consequently also its involvement in transcription.

2.6 Cell cycle arrest induces NF-κB-dependent gene expression only slightly

To further analyse the influence of the cell cycle on NF-κB-dependent gene expression, we tested whether the different cell cycle arrests would induce basal levels of NF-κB-dependent gene expression and whether the cells would still be stimulatable by LPS. In order to answer these questions we analysed the IP-10 mRNA levels of unsynchronized unstimulated, synchronized unstimulated and synchronized stimulated shMock RAW 267.4 macrophages (Fig. 11).

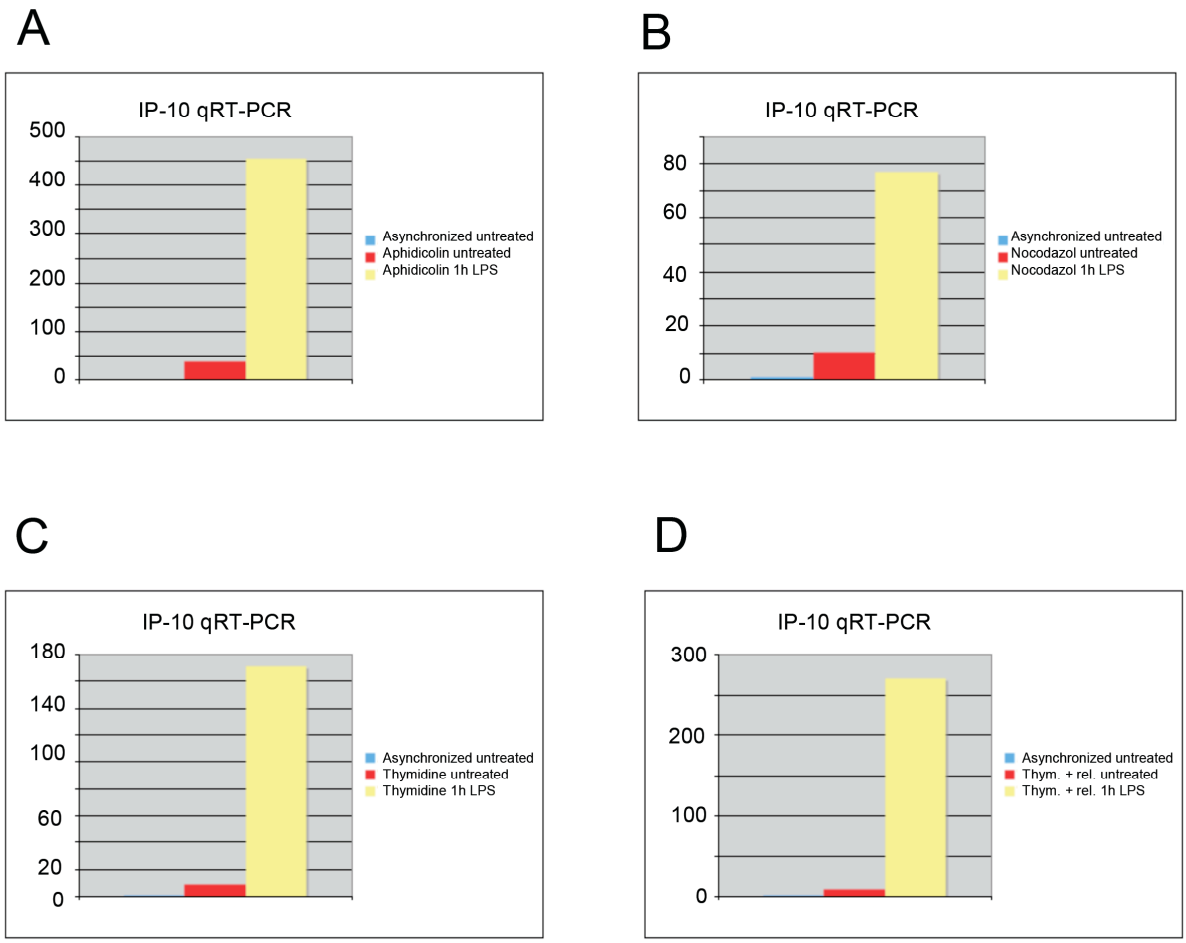

Figure 11: IP-10 gene expression of cells differentially synchronized and subsequently stimulated by LPS (A = Aphidicolin, B = Nocodazol, C = Thymidine or D = Thymidine and release).

While the basal IP-10 mRNA levels were only slightly elevated after Aphidicolin, Thymidine, Thymidine and release or after Nocodazol treatment (10 to 40 fold), additional stimulation by LPS for 1 hour resulted in combination with Aphidiclin treatment in a very strong 450 fold IP-10 induction. An additional stimulation of 80 to 250 fold was observed for cells treated with Nocodazol, Thymidine or Thymidine and release, respectively. The analysis

of other genes (such as IL-1b, IL-12, Csf2, Lif) confirmed the same pattern of gene expression as indicated in Fig. 10 (data not shown). Together, these data provide strong evidence, that the different cell cycle arrests induced NF-κB only slightly and that a subsequent LPS stimulation was able to induce a significant upregulation of the tested NF-κB target genes.

2.7 PARP1 is a transcriptional co-repressor for IL-1b, IL-12 and Csf2 gene expression throughout the cell cycle

The established cell cycle synchronization protocol allowed us to further investigate the transcriptional role of PARP1 during cell cycle. shMock and shPARP1 cells were individually synchronized and additionally treated with LPS (where indicated). After LPS treatment, total mRNA was isolated and analysed by qRT-PCR.

Gene expression analysis of IL-1b, IL-12 and Csf2 revealed that in unsynchronized cells PARP1 functions as co-repressor, since knockdown of PARP1 resulted in an increased gene expression and fold induction (Fig. 12, 13, 14). Synchronization with Thymidine, Thymidine and release or Nocodazol treatment did not change inducibility pattern of the tested genes (compared to unsynchronized cells), suggesting that PARP1 function also in G1/S and G2 as co-repressor (Fig. 12, 13, 14).

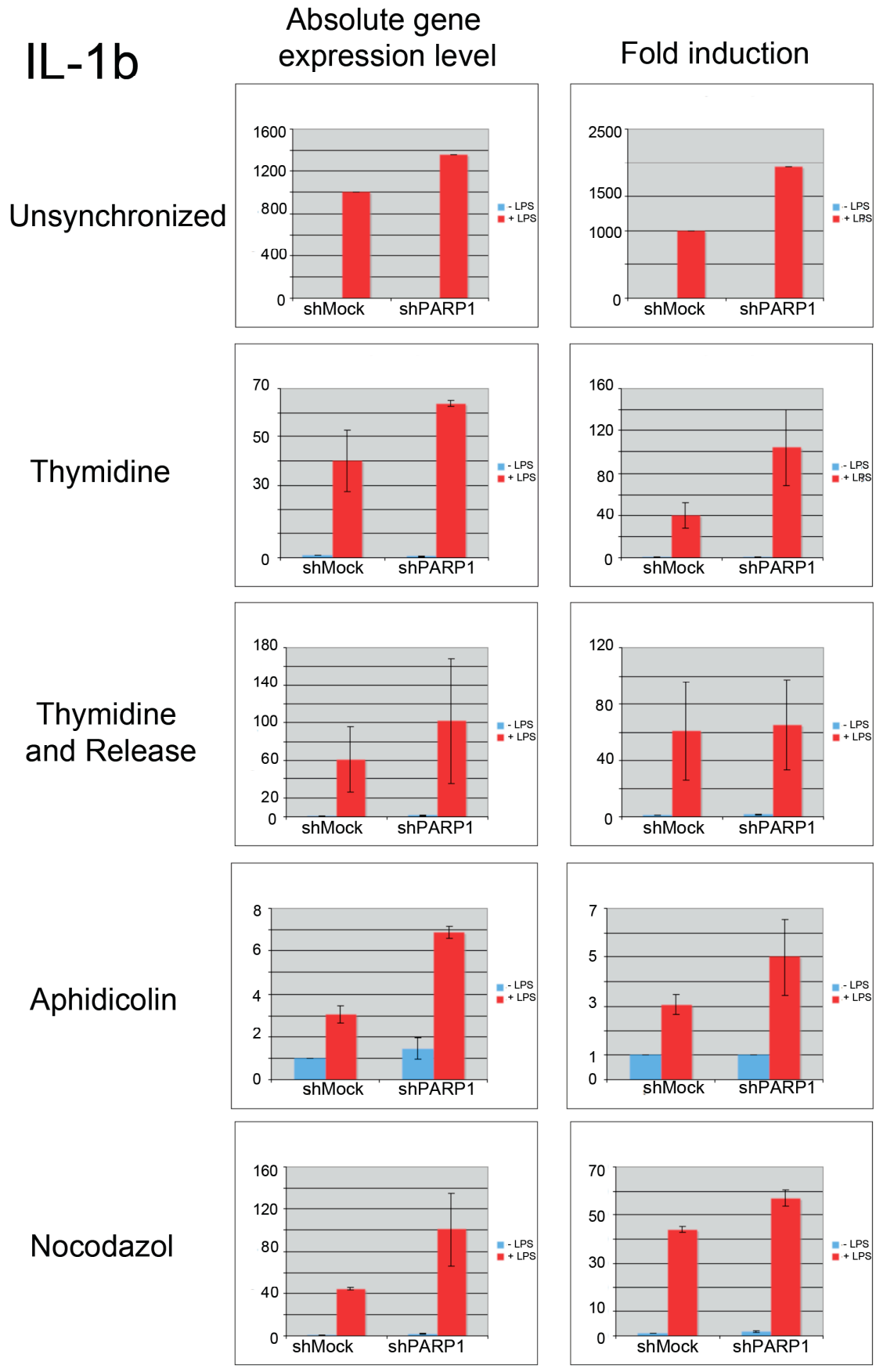

Figure 12: Absolute gene expression levels and fold induction values for IL-1b were analysed by qRT-PCR after the different synchronisation treatments. Standard error bars are calculated from 2 or 3 biological replicates and additional 2 or 3 techniques replicates.

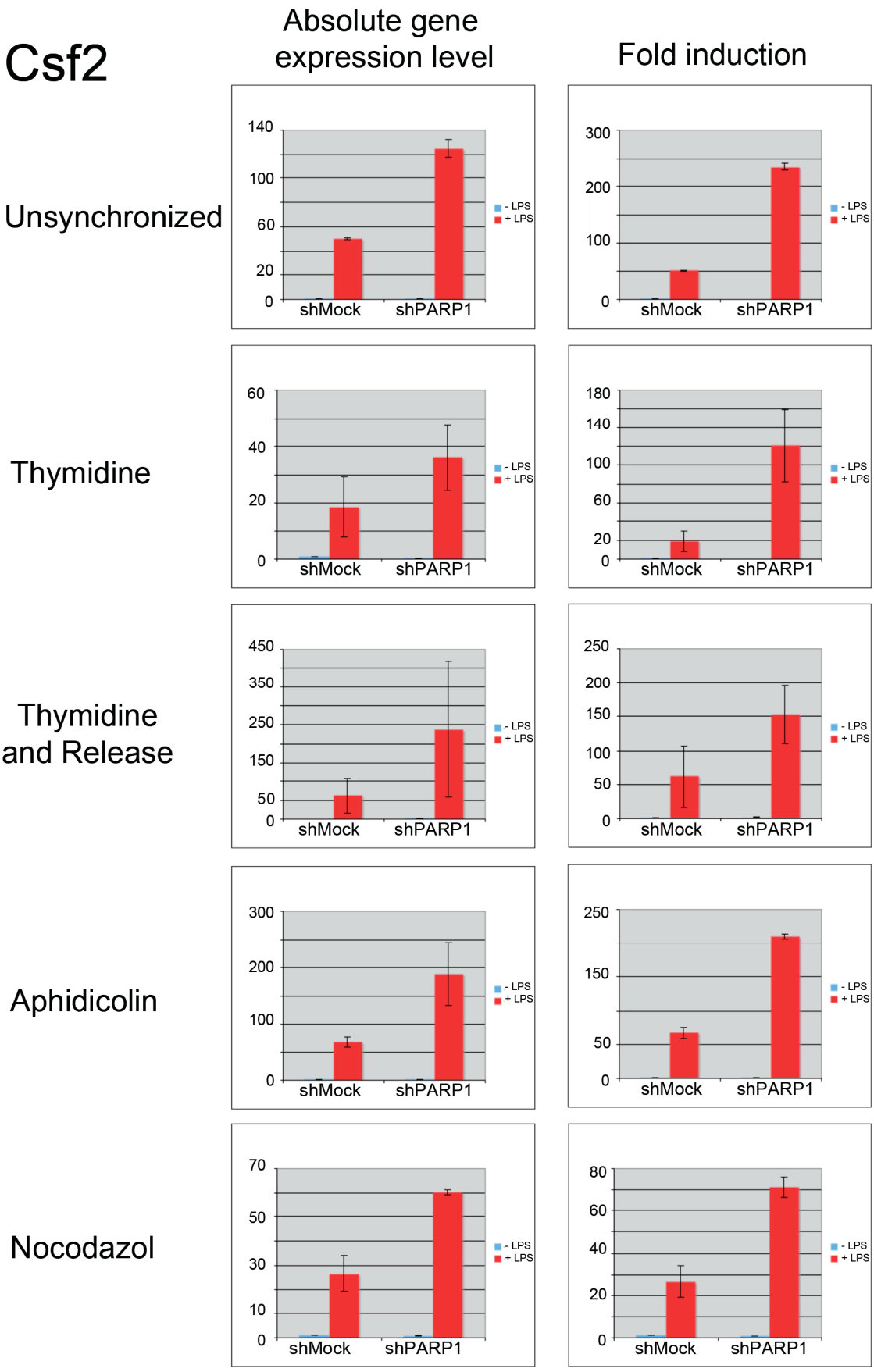

Figure 13: Absolute gene expression levels and fold induction values for Csf2 were analysed by qRT-PCR after the different synchronisation treatments. Standard error bars are calculated from 2 or 3 biological replicates and additional 2 or 3 techniques replicates.

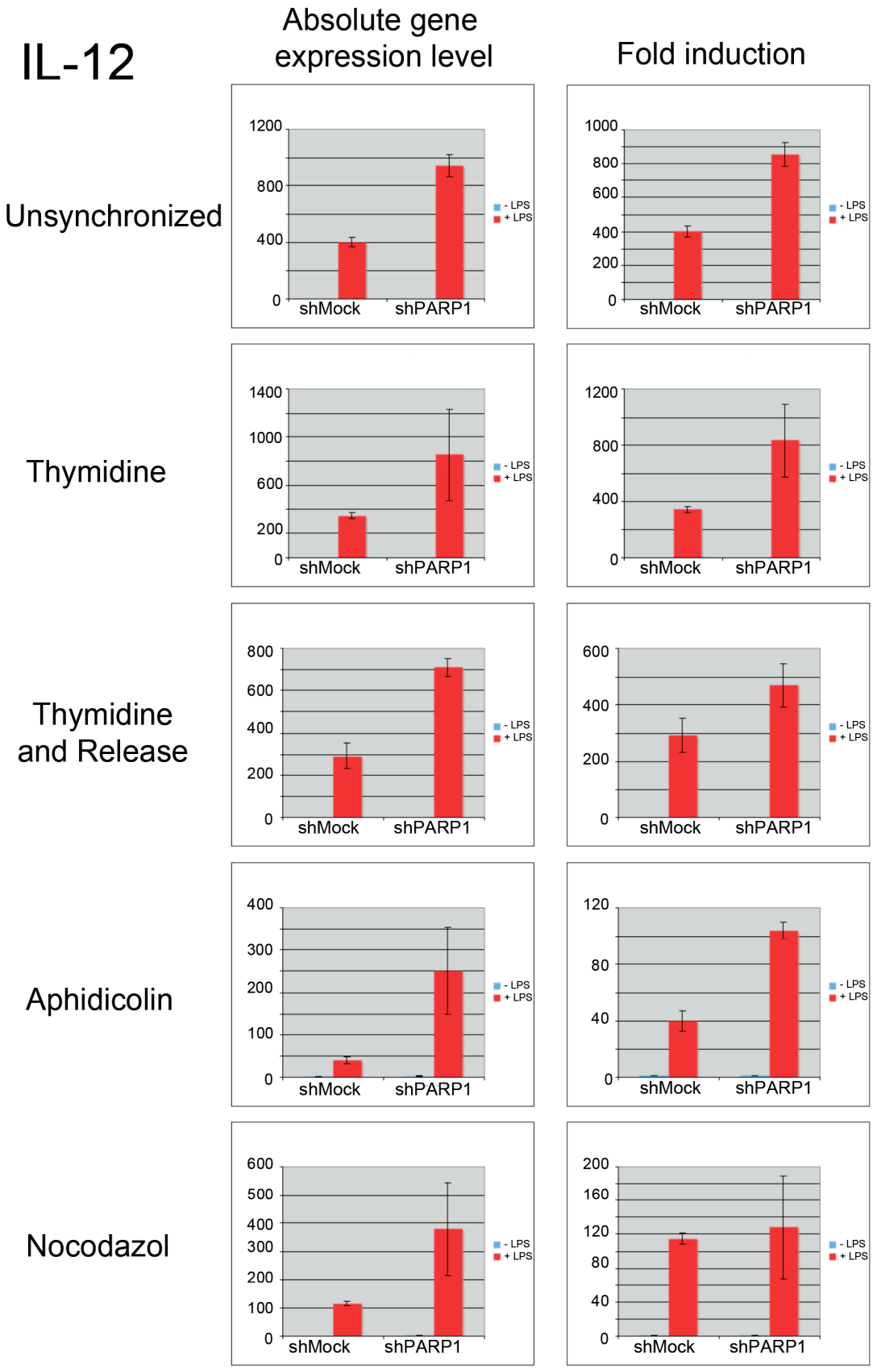

Figure 14: Absolute gene expression levels and fold induction values for IL-12 were analysed by qRT-PCR after the different synchronisation treatments. Standard error bars are calculated from 2 or 3 biological replicates and additional 2 or 3 techniques replicates.

Comparison of the gene expression levels from unsynchronized and synchronized stimulated shMock cells revealed that cell cycle arrest affected gene induction, however in different ways. While for IL-1b the stimulation was very high (1000 fold induction in unsynchronized cells), synchronization of cells reduced the values strongly (down to 40 and 60 fold). Remarkably, the inducibility of Csf2 went up slightly from 50 to 60 fold upon Thymidine and release treatment, suggesting that cells under these conditions are better stimulatable compared to unsynchronized cells. For IL-12 cells treated with Thymidine and Thymidine and release showed a quiet high fold induction (between 330 and 350 fold), only the Nocodazol treatment reduced fold induction.

Together, these results suggest that PARP1 is a transcriptional co-repressor for NF-κB-dependent gene expression of IL-1b, IL-12 and Csf2.

2.8 PARP1 is a transcriptional co-activator in unsynchronized cells, but a co-repressor during G1/S phase for IP-10 gene expression

Analysis of IP-10 gene expression revealed that in unsynchronized cells PARP1 functions in contrast to the other so far analysed cells as co-activator, since knockdown of PARP1 in the shPARP1 cells resulted in a reduced gene induction (Fig. 15).

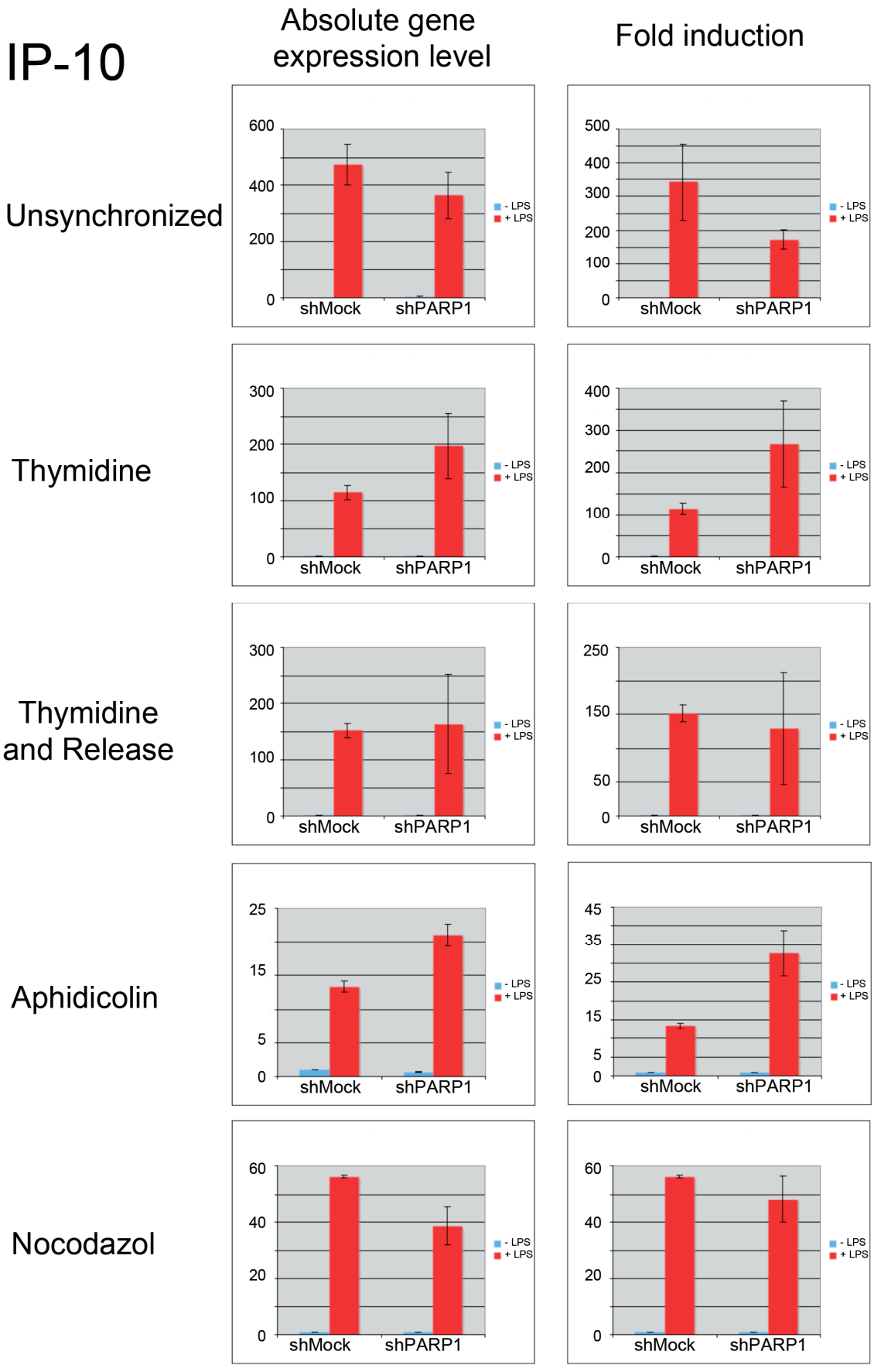

Figure 15: IP-10 gene expression levels and fold induction values were analysed by qRT-PCR upon different synchronisation treatments and LPS stimulation. Standard error bars are calculated from 2 or 3 biological replicates and additional 2 or 3 techniques replicates.

Surprisingly, synchronization with Thymidine reversed the stimulation pattern, suggesting that PARP1 would function as co-repressor under these conditions. Upon Thymidine treatment and release, no difference in IP-10 gene expression levels and fold induction could be detected. Nocodazol on the other hand restored the expression pattern to the one observed in unsynchronized cells. Interestingly, the overall IP-10 gene expression levels were significant reduced after having arrested the cells in the different phases (480 fold for unsynchronized cells, versus approximately 100 fold upon Thymidine treatment or 40 fold after Nocodazol treatment). The reduced induction was not due to increased basal levels.

Together, these results suggest that PARP1 does regulate IP-10 gene expression in a cell cycle-dependent manner. While in unsynchronized cells and cells arrested at G2/M phase, PARP1 acts as co-activator, PARP1 would act in early G1/S phase as co-repressor which would again change 3 hours later in middle of S phase, where gene expression levels seem not to be dependent on PARP1.

2.9 PARP1 is a transcriptional co-repressor in unsynchronized cells, but a co-activator during S phase for Mpa2l gene expression

ShMock and shPARP1 cells were also analysed for LPS induced Mpa2l gene expression. This analysis revealed that in unsynchronized cells PARP1 would function comparable to IL-1b, Csf2 and IL-12 as co-repressor, since knockdown of PARP1 resulted in an increased gene expression and fold induction (Fig. 16). However, synchronization with Thymidine, Aphidicolin and Nocodazol treatment reduced PARP1 dependency since after these treatments no gene expression differences could be observed (Fig. 16). Surprisingly, after Thymidine and release treatment, PARP1 would function as transcriptional co-activator, since the gene expression values were lower when shPARP1 cells were used.

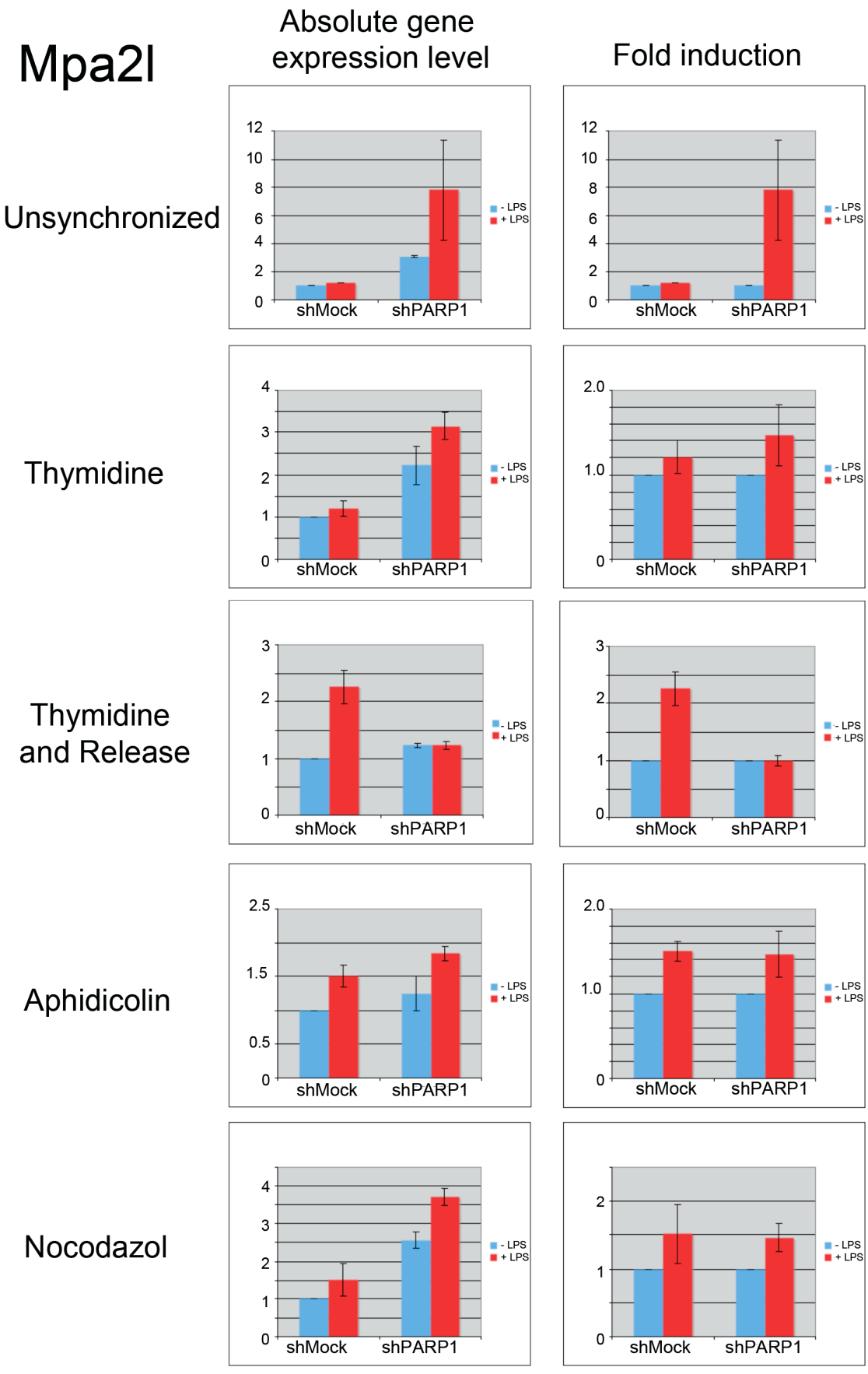

Figure 16: Absolute gene expression levels and fold induction values for Mpa2l were analysed by qRT-PCR after the different synchronisation treatments. Standard error bars are calculated from 2 or 3 biological replicates and additional 2 or 3 techniques replicates.

Togheter, these results suggest that PARP1 does regulate Mpa2l gene expression in a cell cycle-dependent manner. While in unsynchronized cells PARP1 acts as co-repressor, it acts as co-activator in middle S phase. During G1/S and G2/M phase, NF-κB-dependent gene expression is PARP1 independent.

2.10 Lif gene expression is independent of PARP1 in unsynchronized cells, but during G1/S phase PARP1 acts as co-activator

Gene expression analysis revealed earlier, that Lif gene expression was independent of PARP1 in unsynchronized cells. Repeating the analysis for Lif gene expression with synchronized cells revealed, that after the Thymidine and Nocodazol treatment the gene expression levels and fold induction values are explicitly increased for shMock cells compared to shPARP1 cells (Fig. 17), suggesting that PARP1 acts as co-activator. Surprisingly synchronization with Thymidine and release reversed the stimulation pattern, suggesting that PARP1 functions under these conditions as co-repressor.

These data suggest that PARP1 would function during the cell cycle as co-activator as well as co-repressor and that the result obtained with unsynchronized cells represents the sum of all phases.

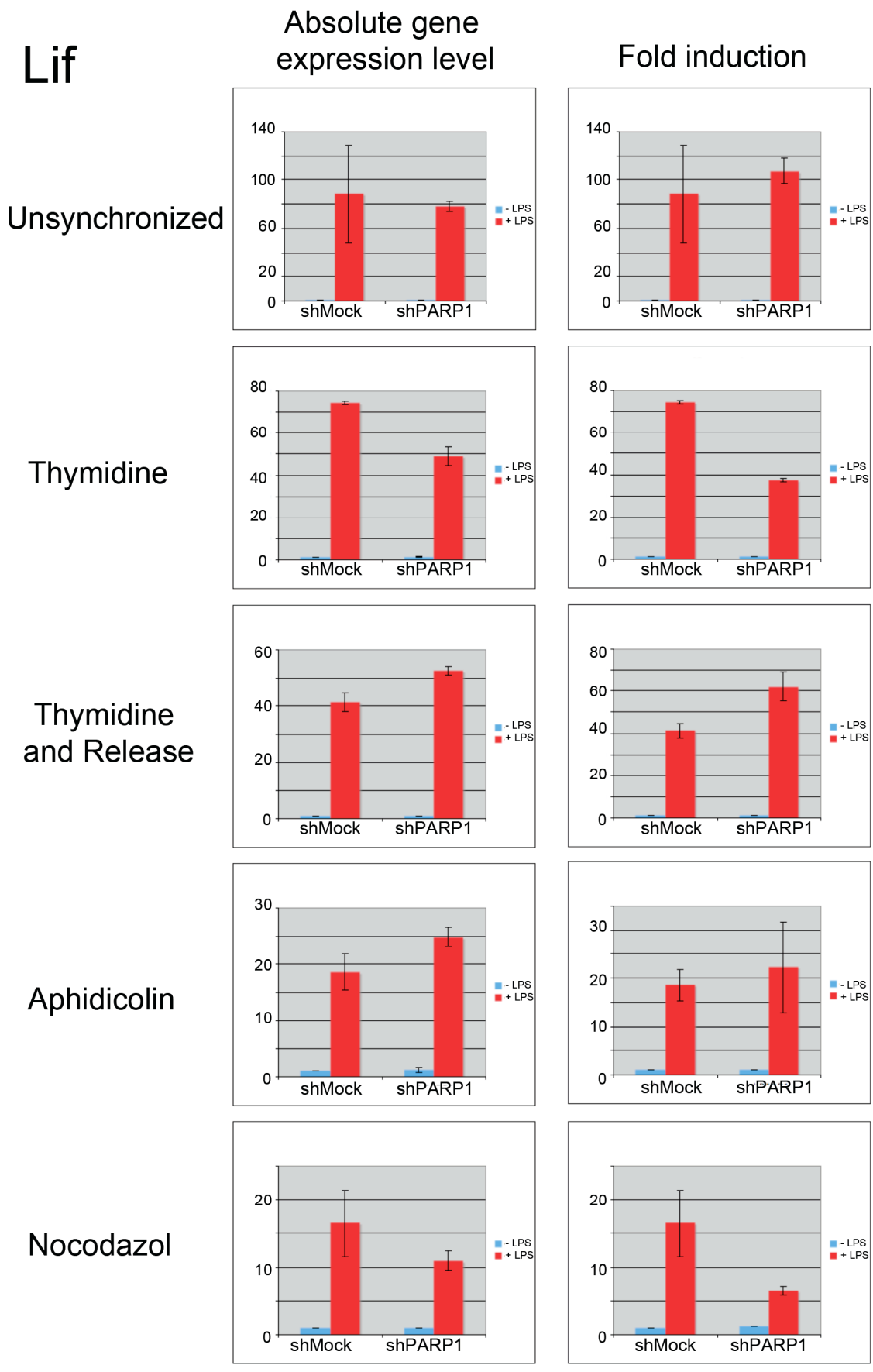

Figure 17: Absolute gene expression levels and fold induction values for Lif were analysed by qRT-PCR after the different synchronisation treatments. Standard error bars are calculated from 2 or 3 biological replicates and additional 2 or 3 techniques replicates.

3 Discussion

The aim of this thesis was to investigate the possible involvement of PARP1 in NF-κB-induced gene expression during cell cycle. LPS activated several NF-κB target genes in RAW 267.4 macrophages, identifying these cells as valuable tool. Retroviral transduction of the RAW 267.4 macrophages allowed the integration and expression of either a shRNA construct directed against PARP1 or a scrambled construct (as control). PARP1 protein levels were subsequently significantly reduced using the short hairpin (sh) RNA approach. Analyses of NF-κB target gene expression after LPS stimulation revealed that dependent on the analysed gene, PARP1 acts either as co-repressor or as co-activator. Treatment of these cells with different chemical compounds, such as Aphidicolin, Thymidine or Nocodazol synchronised cells at different phases of the cell cycle, while only a small amount of the cells (less than 8%) died due to the treatment. Furthermore, cell cycle arrest induced NF-κB-dependent gene expression only slightly, while subsequent LPS stimulation was able to substantially induce an additional upregulation of several tested NF-κB target genes. Interestingly, knockdown of PARP1 did not affect synchronisation. Further analysis of PARP1, however, revealed that cell cycle synchronization induced PAR formation, although PARP1 protein levels were not changed. Cell cycle-dependent analyses of several LPS-induced NF-κB-target genes in unsynchronized cells revealed that PARP1 again would have a dual function. PARP1 acted as co-repressor for Csf2, IL-1b and IL-12 which was not influenced by cell cycle synchronization. For two tested genes, i.e. IP10 or Mpa2l, PARP1 acted as co-activator (IP-10) or as co-repressor (Mpa2l) in unsynchronized cells, which however changed upon the corresponding synchronization of the cells to the opposite type of function. In Thymidine (early S phase) and Aphidicolin (early S phase) treated cells, PARP1 acted as co-repressor for IP10 and in Thymidine and release (early S phase) treated cells, PARP1 acted as co-activator for Mpa2l. In unsynchronized cells, gene expression for Lif is PARP1 independent, while after Thymidine (early S phase) and Nodocazol (G2/M) treatement, PARP1 acted as co-activator.

While genes such as IL-1b, IL-12, and IP-10 were reproducibly induced to a high degree, no induction was observed for other genes such as IL-15, a previously described NF-κB target gene (86). Given that LPS induced other genes, and that the primer per se were functioning (judged by the production of only one single PCR product, confirmed by the melting curve and by agarose gel electrophoresis), we concluded that the IL-15 gene was after

LPS treatment for 1 hour not or only very weakly induced in the tested Raw macrophages. The reason remains to be elucidated.

The observed contribution of PARP1 in NF-κB-dependent gene expression never reached 100% (i.e. complete loss of gene expression) which could be explained by the fact, that although PARP1 levels could not anymore be detected by western blot analysis in the shPARP1 treated cells, there was a rest amount of PARP1 molecules which would interfere with our analysis. Furthermore, we cannot exclude that other PARP family members might functionally complement the loss of PARP1 in the shPARP1 macrophages.

Strikingly, PARP1 functions for some genes in unsynchronized cells as transcriptional co-activator, and as co-repressor for others. The association of PARP1 with the chromatin could possibly explain the two opposing functions. Depending on the nucleosomal environment around the transcription start site (e.g. nucleosomal positioning or modification of the histone tails), PARP1 might either increase the accessibility for NF-κB to its response element and thus enhance gene expression or, alternatively, reduce NF-κB DNA binding and subsequently the extent of gene expression. Especially the repressor function of PARP1 would guarantee that pro-inflammatory cytokines are not strongly expressed, which would be detrimental for the organism. An alternative explanation would be, that PARP1 would act as promotor-specific exchange factor which would recruit to the transcriptional start site either co-activator or co-repressor complexes, as it was suggested for the activation of specific neurogenic gene programs (87). PARP1 might regulate NF-κB-dependent gene expression dependent on the exposure time of a cell to LPS, which could be part of a negative feedback loop and help to attenuate harmful gene expression. For some “early” genes such as Csf2 and IL-12, the putative negative feedback might already be activated after one hour LPS stimulation, while for “late” genes such as IP-10 it might take longer to activate the postulated negative feedback. This hypothesis is further supported by the fact, that after 4h LPS stimulation also for IP-10 a co-repressor activity for PARP1 was observed (data not shown). The same switch was also observed after different times of LPS stimulation. Whether this feedback mechanism holds true, has to be tested for more genes and also including different other stimuli.

Gene expression analyses of unsynchronized cells are always the sum of the expression profiles of cells in the different phases. It can be easily foreseen, that gene expression during S phase is additionally influenced by the replication machinery of the cell and possibly by the modification of the chromatin, which is required to replicate the DNA. To elucidate mechanistic regulation by proteins on transcription, it is thus important to also

analyze gene expression in distinct phases of the cell cycle. To simplify our analysis, we decided to analyze RNA from cell cycle synchronized samples only 1 hour after LPS stimulation. Chemical compounds arrested the cells to the similar extent in the desired phase, independent PARP1 being present or knocked down, suggesting that PARP1 is not required for the arrest of cells at defined phases. On the other hand cell cycle arrest induced NF-κB-dependent gene expression only slightly and still allowed further stimulation by LPS.

The differential observed contribution of PARP1 in gene expression (co-activator or co-repressor) was not only observed in a gene-type and induction time specific manner, but was also observed for a defined gene such as IP10, Mpa2l or Lif in a cell cycle-dependent manner (for a given gene at 1 hour LPS stimulation). These results suggest that the cell cycle does influence PARP1 and consequently also PARP1-dependent gene expression. Since the synchronization of cells also induced the enzymatic activity of PARP1 (but not its protein levels), the observed changes might be dependent on the treatment. The enzymatic activity of PARP1 was earlier described to be important for the remodeling of the chromatin structure (18). On the other hand, our laboratory provided earlier evidences, that the enzymatic activity of PARP1 was not required for transcriptional activation of transiently transfected reporter genes (22). The fact that PARP1's function was not changed for all genes to the same extend and in the same cell cycle phase (e.g. always changing in Thymidine treated cell), suggests that there might exist an additional so far unrecognized level of PARP1's involvement in transcriptional regulation. Furthermore, experiments with cells synchronized by other growth arrest, revealed that PARP1 forms PAR polymers upon entering the S phase (personal communication, Suheda Erener) suggesting that the observed enzymatic activity of PARP1 might in part still be physiological relevant. This theory would be supported by the fact that some cell cycle activities are influencing PARP1 (85). One mechanism to activate PARP1, also in a DNA-damage independent manner, would be by post-translational modification. PARP1 was recently described to be phosphorylated by different kinases (88).

Together our results provide strong evidences for the involvement of PARP1 in NF-κB-dependent gene expression during the cell cycle, although the mechanisms regulating these processes have to be further elucidated. Whether these results are also valid and observed when cells are stimulated with other NF-κB inducing stimuli and found in other cell types has also to be further analyzed.

Outlook and medical relevance

It is proposed that the finding, that PARP1 has a cofactor function for NF-κB, might help to design new therapeutic strategies for treatment of inflammatory disorders, based on the combined pharmalogical inhibition of NF-κB and PARP1 interaction (58). A variety of widely used anti-inflammatory agents inhibit the NF-κB pathway, resulting in a decrease in NF-κB-dependent transcription (89). However, blocking the NF-κB pathway for prolonged periods is not feasible, since NF-κB plays an important role in the maintenance of the host defense responses. Moreover, since PARP inhibitors are not only able to inhibit the enzymatic activity of PARP1 but also other PARPs, complete long-term inhibition of the enzymatic activity of PARP1 might lead to severe side effects. Therefore, the NF-κB/PARP1 interface might be an obvious target for the development of new types of drugs disrupting specific protein-protein interactions during the whole cell cycle. Taken together, future investigations of the various roles of PARP1 in transcription and signaling under pathophysiological conditions *in vivo*, will certainly represent an intense exciting field of research (1).

4 Material and Methods

4.1 Material

4.1.1 Cell lines

All experiments were performed with RAW 264.7 macrophages. These are mouse monocytes/macrophages originally isolated from a mouse tumor induced by a Abselon Leukaemia virus. PARP1 knockdown was achieved by retroviral transduction of cells with (bistronic self-inactivating) lentiviral vector expressing sh(short hairpin)RNAs directed against PARP1 mRNA, which resulted in a stable reduction of PARP1 protein levels. Control cells were transduced with a retroviral shMock RNA construct.

Adherent Raw 267.4 macrophages were grown in RPMI medium in the presence of 10% fetal calf serum (FCS) and penicillin (50U/ml)/streptomycin (50µg/ml). Cells doubled approximately every 24 hours and were split 1:3 when they reached 90% confluence.

4.1.2 Solutions

Solutions for cell culture

Medium:	GIBCO® RPMI 1640 Medium (1X), liquid, with L-Glutamine (Invitrogen) Supplemented with 10% fetal calf serum (FCS) (Invitrogen), 50U/ml Penicilllin (Invitrogen) and 50µg/ml streptomycin (Invitrogen)
PBS (10x)	1.37M NaCl 100mM $Na_2HPO_4 \bullet H_2O$ 30mM KH_2PO_4 ad 1L H_2O adjust PH 7.4 (with HCl)

Solutions for the generation of whole cell extracts

Lysis Buffer:	50mM Tris/HCl pH 7.5 400mM NaCl 25mM NaF 1% (v/v) Triton X-100

Solution to define protein concentrations:

5x Bradford Solution	BIO-RAD Protein Assay (Bio-Rad Laboratories GmBH)
Standard proteins	bovine serum albumin, homemade in the own lab (concentrations: 0.2, 0.36, 0.54 and 0.72 mg/ml)

Solution for SDS-Polyacrylamide Gel Electrophoresis (SDS-PAGE)

Running buffer	1.5M Tris pH 8 0.4% (w/v) SDS
Separation Gel (10%)	4ml ddH_2O 2ml Solution B 2ml 40% acrylamide solution 0.08ml 10% APS 0.008 ml TEMED
Solution B	1.5 M Tris /HCl pH 8.8 0.4% Na-dodecylsulfate (SDS) ad 200ml ddH_2O
Stacking Gel (4.8%)	3.15 ml ddH_2O 1.25 ml Solution C 0.6 ml 40% acrylamide solution add immediately before use:

	0.05 ml 10% APS 0.005 ml TEMED
Solution C	0.5 M Tris/HCl pH 6.8 0.4% Na-dodecylsulfate (SDS) tipfull Bromphenol blue ad 200ml ddH_2O
40% Acrylamide Solution	Acrylamid-Bis (solution (37.5:1), 40% (w/v)), SERVA biosystems GmBH
10x protein loading buffer	600mmol/l Tris-HCL pH 6.8 20% Na-dodecylsulfate 20% Glycerol 0.05% Bromphenol blue 20% Mercaptoethanol 25mmol/l DTT

Solutions for Western Blot analysis

Transfer buffer (5x)	250 mM Tris-HCl, pH 8.6 1.92 M glycin
Transfer buffer (1x)	20 % (v/v) 5x blotting buffer 10 % (v/v) methanol
TBS	10mM Tris/HCl pH 7.5 150mM NaCl
TBS-T	10mM Tris pH 8 150mM NaCl 0.1% (v/v) Tween-20

ECL solution A	Uplight HRP blot Reagent A (UP99619A-A), luminal/enhancer solution, Uptima Interchim
ECL solution B	Uplight HRP blot Reagent B (UP99619A-B), oxidizer solution, Uptima Interchim

4.1.3 Antibodies

Anti-PARP1	rabbit, immunization of rabbit made at UZH
Anti-PAR (LP96-10)	rabbit, alexis biosience, 210-890-R100
Anti-Tubulin	mouse, Sigma, T6199
Anti-GAPDH (FL-335)	rabbit, Santa-Cruz, sc25778

Secondary antibodies:

Anti-rabbit	ECL TM Anti-rabbit IgG, horseradish Peroxidase linked whole antibody (from donky), NA934V, GE Healthcare UK Limited
Anti-mouse	ECL TM Anti-mouse IgG, horseradish Peroxidase linked whole antibody (from sheep), NA931V, GE Healthcare UK Limited

4.1.4 Kits and enzymes

RNA isolation	Agilent Total RNA Isolation Mini Kit, Agilent Technologies
Reverse transcriptions	High Capacity cDNA reverse Transcription Kit, Applied Biosystems
RT-PCR	GoTag polymerase, Promega
Syber Green	Sensi Mix^{TM} Plus SYBR®, Quantace

4.1.5 Chemicals

Stimulation

LPS	LPS (Lipopolysaccharides) from Escherichia coli055:B5 (Sigma, L2880) was used. The LPS powder was aliquoted in 5mg/ml in PBS in Eppendorf tubes and stored at -20°C.
TNF-α	Recombinant TNF-α was produced in the own laboratory.

Cell synchronization

Thymidine	99-100%, Sigma-Aldrich, T1895
Aphidicolin	from Nigrospora sphaerica, minimum 98%, Sigma-Aldrich, A0781, liquid Aphidicolin was aliquoted in 5mg/ml in DMSO.
Nocodazol	≥99% (TLC), powder, Sigma-Aldrich, M1404

DNA staining FACS preparation

Propidium Iodid	Propidium Iodide solution, 1mg/ml in water, Sigma-Aldrich, P4864
RNase	RNase A, from bovine pancreas, Roche, 10 109 169 001

4.1.6 Primer

The primers were designed using several programs from the internet. The sequence of the gene was taken from the Genbank (http://www.ncbi.nlm.nih.gov/). The exon and intron informations were taken from (http://www.ensembl.org/index.html). Primers were self designed or suggested by the primer request program (http://eu.idtdna.com/Scitools/Applications/PrimerQuest/Default.aspx/?c=EU) and then the primer sequences were analysed using primer analyse programs

(http://eu.idtdna.com/analyzer/Applications/OligoAnalyzer/) and oligocalc (http://www.basic.northwestern.edu/biotools/oligocalc.html).

Forward and reverse primers would bind to 2 different exons with an intron in between, typically larger than 3kb. Even better, the primers would cover an exon-exon boundary. The primers were designed such that their annealing temperature was about 60°C and with a 100-200 bp product. The difference in annealing temperature between forward and reverse primer was never larger than 1°C. The GC content was between 40 and 60 %. Never more than 2 or 3 G/C were at the 3'end and runs of the same nt were avoided. In order to minimize self-dimer and hetero-dimer (primer-dimer) formation, the delta G of primer dimers was never smaller than -6kcal/mol. The secondary structure of the template was checked with the mfold program (http://frontend.bioinfo.rpi.edu/applications/mfold/cgi-bin/dna-form1.cgi) and hairpins were avoided.

Primers were ordered from Sigma-Aldrich and first a control run with RNA dilutions from 1 to 1: 10 000 in 10fold steps was done and afterwards an agarose gel was run with the qRT-PCR products to confirm the amplification of only 1 PCR product. The usefulness was defined on the basis of the melting curve and the agarose gel results.

Primers were ordered from Sigma-Aldrich.

Gene	Forward sequence
	Reverse sequence
IL-1b	5'-GAAGAAGAGCCCATCCTCTGTG-3'
	5'-GCTCATGGAGAATATCACTTGTTGG-3'
IL-12b	5'-CAACATCAAGAGCAGTAGCAGTTCC-3'
	5'-CAGGTGACATCCTCCTGGCAG-3'
IL-15	5'-GACAGTGACTTTCATCCCAGTTGC-3'
	5'-GCAGCCAGATTCTGCTACATTCTTG-3'
TNF alpha	5'-GTCGTAGCAAACCACCAAGTGG-3'
	5'-GAGATAGCAAATCGGCTGACGG-3'
Hif1an	5'-CTCATTGGCATGGAAGGAAATGTGAC-3'
	5'-TGTCAAAGTCCACCTGGCTCTG-3'
IP-10	5'-GCACGAACTTAACCACCATCTTCC-3'
	5'-CTACCCATTGATACATACTTGATGACAC-3'
Mpa2l	5'-GATGCTGAAGAAGCTAATGAAGGATC-3'

	5’-CCTTGATGACATCTCTCAGTTGCTG-3’
Lif	5’-CCATAGATGCAGCAAGGAGA-3’
	5’-CAGTCCTGAGATGAGCCTGA-3’
Csf2	5’-ACATGCCTGTCACGTTGAAT-3’
	5’-TTGAGTTTGGTGAAATTGCC-3’
PARP1	5’-GCAGTCACCCATGTTCGATGG-3’
	5’-GCTTCTCTGGATCCACCATC-3’
GAPDH	5’-GCTACACTGAGGACCAGGTTG-3’
	5’-GCCCCTCCTGTTATTATGGGGG-3’
PARP2	5’-CCTAACAGGATGCTGCTCTGG-3’
	5’-GCTACCTCTGACAGAAGAAGC-3’

4.2 Methods

4.2.1 Culturing of cells

Cell culture work was performed under a sterile hood. Cells were cultured as adherent monolayer on 10 cm cell culture dishes. Cells were growm in a cell incubator at 37 °C and 5% CO_2.

To split cells, old medium was aspirated and cells were washed once with 10 ml PBS for 10 seconds. After aspirating the PBS, 3 ml new medium was added. Cells were scraped off the plate using a cell scraper, and resuspended in the medium by pipetting them 5 times slowely up and down. Finally, 1ml was transferred to a new dish, which was prepared with 10 ml new medium. To determine the exact cell numbers, cells were counted in the Neubauer-counting chamber.

4.2.2 Freezing of cells

Cells from a 80% confluent 10cm dish (corresponding to approximately 5 x 10^6 cells) were washed once with 10 ml PBS. 1ml DMSO-FCS solution (10% DMSO, 90% FCS) was added to the cells, which were subsequently scraped off the plate and resuspended by pipetting them 5 times. Then they were transferred to a cryo-vial. The vial was first stored for one night at -80°C in a cryo-box with isopropanol and afterwards stored in liquid nitrogen.

4.2.3 Thawing of cells

Cryo-vial were thawed in a 37°C water bath. As soon as the whole ice was thaw, the cells were transferred in a prepared 15ml Falcon tube with 5 ml warm medium. After spinning down for 3 minutes at 1000rpm, the cell pellet was dissolved in 1 ml medium and transferred in a new 10cm dish prepared with 10 ml fresh medium. The following day, the medium (containing 10% FCS) was changed.

4.2.4 Stimulation of cells with LPS/TNF-α

LPS (10μg/ml) or TNF-α (100ng/ml) was directly added in the medium. The dish was holded transversely and then carefully shaked.

4.2.5 Cell synchronization

To synchronize cells, 1.5 x10^6 cells/ml were seeded in a 10 cm dish and incubated for 24h at 37°C and 5% CO_2. After 24h the cells were adherent and approximately at 40 - 50% confluence. After washing with 10 ml PBS, 6 ml new medium containing the according synchronization compound was added. After the chosen duration with the synchronization compound in the incubator and after the LPS stimulation (description see above), cells were prepared for FACS analysis, protein or RNA isolation.

Attached time protocols were followed for each experiment:

For Aphidicolin

First day: 6–7 PM, seeding of total 1.5 x10^6 cells

Second day: 7 PM, Aphidicolin application (5μg/ml), 14h block

Third day: 8 AM, LPS stimulation, cells fixed for first control by FACS

9 AM, RNA isolation, cells fixed for second control by FACS, protein isolated (only shMock cells)

For Nocodazol

First day: 5-6 PM, seeding of total 1.5 x10^6 cells

Second day: 6 PM, Nocodazol application (0.4μg/ml), 15h block

Third day: 8 AM, LPS stimulation, cells fixed for first control by FACS

9 AM, RNA isolation, cells fixed for second control by FACS, protein isolated (only shMock cells)

For Thymidine

First day: 5-6 PM, seeding of total 1.5 x10^6 cells

Second day: 6 PM, thymidine application (0.6mg/ml), 15h block

Third day: 8 AM, LPS stimulation, cells fixed for FACS analysis

9 AM, RNA isolation, cells fixed for FACS analysis, protein isolated (only shMock cells)

For Thymidine with 3 hours release:

First day: 5-6 PM, seeding of total 1.5 x10^6 cells

Second day: 6 PM, thymidine application (0.6mg/ml), 15h block

Third day: 8 AM, wash 3 times with 10ml PBS, new Medium without thymidine

10 AM, LPS stimulation, cells fixed for FACS analysis

11 AM, RNA isolation, cells fixed for FACS analysis, protein isolated (only shMock cells)

4.2.6 DNA staining with Propidium Iodide

For adherent cells the medium from a 40 - 50% confluent 10 cm dish (containing approximately 2× 10^6 cells) was aspirated and the cells were trypsinized with 1.5 ml trypsin on the plate for 5 minutes. Swimming cells were first spun down for 3 minutes at 1100rpm. The medium was aspirated and the cell pellet was subsequently dissolved with 1ml trypsin for 30 seconds. The trypsin-cell-mixture was transferred in a FACS tube containing 3ml Medium to inactivate the Trypsin. Cells were spun down for 3 minutes at 1100 rpm by 4°C, afterwards the cell pellet was washed with 2 ml cold PBS and again spun down for 3 minutes at 1100rpm at 4°C. After aspirating PBS, the cell pellet was very well dissolved in 300µl cold PBS. Cells were fixed in 70% ethanol by adding during vortexing drop by drop 700µl 100% Ethanol (-20°C). For complete fixation, FACS tubes were left for 30 minutes on ice. Or cells could be stored up to 1 week at 4°C. Fixed cells were spun down for 5 minutes at 1200rpm at 4°C, the supernatant containing 70% ethanol was discarded, and the cell pellet was dissolved in 2 ml cold PBS before an additional round of centrifugation for 5 minutes at 1200 rpm at 4°C. During this time the Promidium Iodide (PI) Staining Solution was prepared by solving

100µg/ml RNase A and 20µl/ml PI in cold PBS (for 10 samples take 5 ml cold PBS, 250 µl Rnase A (2mg/ml) and 100ul PI (1mg/ml)). After discarding PBS, 500 µl of the Staining Solution with RNase was used to dissolve the cell pellet. For a good DNA staining, cells were incubated in the dark for 30 minutes at 37°C. FACS analysis was performed immediately, although cells could also be stored for one week at 4°C.

4.2.7 FACS Analysis

FACS analysis was performed according to the manufactured protocol. The DNA histograms representing the fluorescence intensity distribution among cells indicate the number of cells per channel in the ordinate and the relative fluorescence intensity which varies in proportion with the DNA content in the abscissa. To facilitate the comparison between different samples in a given figure, the scale of the ordinate was normalized to a predetermined height of 1000 or 1500, if it was useful. For each analysis 100 000 cells were counted.

4.2.8 Generation of whole cell extracts

The medium was aspirated and the cells were washed with 10 ml PBS. 3 ml of fresh medium were added to scrape the cells off the plate by using a cell scraper. The cells were collected in a 15ml Falcon tube and spun down for 3 minutes at 1100 rpm at 4°C. The supernatant was discarded and the cell pellet was washed with 2ml cold PBS. After repeating the centrifugation for 3 minutes at 1100 rpm, 4°C, the cell pellet was resuspended in 1ml cold PBS and the cells were transferred in an eppendorf tube. After spinning down for 3 minutes, at 1100 rpm, at 4°C, the supernatant was aspirated and if preferred, the cell pellet was snap-freezed in liquid nitrogen and stored at -20°C. If proteins were isolated immediately, 100 - 200µl (dependent on the cell pellet size) lysis buffer were added to the cells and the tube was rolled for 30 minutes at 4°C. After centrifugation of the extract for 30 minutes, at 14 000 rpm and at 4°, proteins, which were now in the supernatant, were transferred in a new eppendorf tube.

4.2.9 Bradford Protein Assay

The Bradford protein assay is a spectroscopic analytical procedure used to measure the concentration of protein in a solution. Bradford is a dye, which stains all proteins with equal intensity. The total protein amount is measured. The Bradford Solution (5x) was diluted 5 times with ddH_2O to the desired amount. The standard curve was measured by adding 20 µl of the standard proteins (0.2 mg/ml, 0.36 mg/ml, 0.54 mg/ml and 0.72 mg/ml) to 1ml 1x Bradford Solution. To measure protein of the whole cell extract, 2 µl (or more if needed, the color should at least reach the level from the lowest standard solution) of the extract were mixed with 1ml 1x Bradford Solution. The absorbance was measured at 595nm and the protein concentration of the extract was calculated with help of the standard proteins.

4.2.10 SDS-Polyacrylamide Gel Electrophoresis (SDS-PAGE)

Separation of proteins from a protein mixture by their molecular mass was achieved by sodium dodecyl sulfate (SDS) polyacrylamide gel electrophoresis (PAGE). The anionic detergent SDS denatures proteins and forms negatively charged complexes with constant charge to mass ratios. In an electric field, proteins complexed by SDS migrate according to their charge allowing the separation by molecular weight. Two glass slides (10 x 8.5 cm) were rinsed with deionized water and two distance holders (10 x 0.15 cm) were placed in between them. The slides were put into a gel preparation electrophoresis unit. 8 ml of the separating gel solution were poured between the glass slides and mounted with 70 % (v/v) ethanol. Upon polymerisis of the polyacrylamide gel, the alcohol was removed and the upper border of the separating gel was rinsed several times with deionized water. The stacking gel solution was poured onto the separating gel and a comb with 10 wide or 15 narrow slots was inserted to generate the sample pockets. Polymerized gels could be stored in a wet chamber at 4 °C for up to 3 days.

Before separation, protein samples were adjusted to equal volumes with H_2O, 10x protein loading buffer was added to the samples before they were heated at 95 °C for 5 minutes. The gel chamber of the electrophoresis unit was filled with 1x running buffer, the sample pockets were rinsed with running buffer and samples were loaded into the pockets. 4 µl of a prestained molecular weight marker were loaded in one pocket to follow the separation of the proteins and to control the transfer efficiency of proteins onto nitrocellulose or PVDF membranes upon blotting (see western blot). Samples were allowed to enter the stacking gel at a constant voltage of 80V. When the loading dye front reached the separating gel, the

voltage was increased to 100V. Electrophoresis was typically stopped when the loading dye front had reached the bottom of the gel. After electrophoresis, the gel was removed from the glass slides, the stacking gel was peeled off and proteins in the separating gel were transferred onto a nitrocellulose or PVDF membrane by western blot.

4.2.11 Western Blot analysis

Proteins were separated on a SDS-Gel electrophoresis and electroblotted over night at 30 V onto a nitrocellulose or PVDF membrane in transfer buffer at 4°C. One hour before terminating the voltage was increased to 100 V. The western blot "sandwich" was assembled as followed: black plastic, one sponge wetted in the transfer buffer, 2 filter papers wetted in the transfer buffer, SDS-gel, nitrocellulose or PVDF membrane (the PVDF membrane has first to be activated in 100% methanol for 20 seconds and washed for 1 minute in the transfer buffer; the nitrocellulose membrane on the other hand has only to be wetted for 5 seconds with transfer buffer), 2 filter papers wetted in the transfer buffer, one sponge wetted in the transfer buffer, white or clear plastic. During the sandwich assembly air bubbles between the gel and the membrane were carefully removed by rolling a glass rod over the assembled sandwich. The sandwich was inserted into a western blot chamber, which was cooled with an ice block. The following morning the blotting was completed, the membrane was removed from the blotting chamber and washed in deionized water.

After blocking the membranes for 60 min in TBS-T containing 5% (w/v) milk powder, the membranes were incubated with the appropriate antibodies, diluted in TBS-T with 5% (w/v) milk powder, for 2 hours at room temperature. Then the membranes were washed 3 times for 10 minutes in TBS-T and incubated with the corresponding secondary antibodies, diluted in TBS-T with 5% (w/v) milk powder, for 1 hour. The membranes were subsequently washed 2 times for 10 minutes in TBS-T and additionally 2 times for 10 minutes in TBS. All washing and incubation steps for immunodetection of proteins were conducted on a shaker at room temperature. The membrane was placed on a sarasin transparent sheet and 1 ml of ECL solution (1 ml ECL solution A, 1 drop ECL solution B) were dropped directly onto the membrane. The membrane was exposed to a x-ray film for different time points in the dark before chemiluminescence was detected using a chemiluminescence imager. Exposure times were typically chosen in the range of 1 second to 15 minutes.

4.2.12 RNA Isolation

RNA was isolated directly from cells on plate with the RNA Isolation Kit (Agilent Technologies). To be able to use 600 µl lysis solution for 2 to 3 dishes, it was important, to aspirate the remaining PBS completely, otherwise PBS would interfere with efficient cell lysis. For the further RNA isolation steps the manufactured protocol was followed. To keep RNA after isolation, the samples were snap freezed and stored at -80°C.

4.2.13 Quantification of RNA

RNA was quantified with the NanoDrop spectrophotometer. After blanking and setting the system to zero with 1 µl of destilled water, 1 µl of RNA-sample was placed onto the sensor and the RNA concentration was automatically measured and calulated by the instrument. The NanoDrop ND-1000 Spectrophosphometer (260/280nm) measures 1µl samples with concentrations between 2 ng/µl and 3000 ng/µl.

4.2.14 Reverse Transcription

Reverse transcription was performed with the High Capacity cDNA, Reverse Transcription Kit (Applied Biosystems). To 2 µg isolated RNA different amount of destilled H2O was added (up to 10µl). Subsequently, 10µl of the Master Mix were added, to get a total reaction volume of 20µl. All preparations were done one ice.

Master Mix for 1 sample contained:

2µl	10x RT buffer
0.8µl	25x dNTPs
2µl	10x Primers
1µl	reverse transcriptase (add not until use immediately)
4.2 µl	destilled H2O
10µl	total volume

For the negative reverse transcriptase control (-RT), a Master mix without RT was pipetted. Reverse Transcription was performed in a GeneAmp® PCR System 2700 (Applied Biosystems). PCR protocol was:

10 minutes	25°C
120 minutes	37°C
5 seconds	85°C
∞	4°C

Newly transcribed cDNA was stored at -20°C.

4.2.15 Conventional RT-PCR

Conventional RT-PCR included the previous transcribed cDNA (see above). For a standard PCR, GoTag polymerase (Promega) and self designed primers were used.

GoTag PCR Master Mix:

14.68 µl	ddH20
5µl	GoTagBuffer
1.5µl	GoTag $MgCl_2$
0.2µl	dNTPs (25mM)
0.12µl	GoTag (polymerase)
1µl	forward primer (10µM)
1µl	reverse primer (10µM)
23.5µl	**total volume**
1.5 µl	cDNA
25µl	**total volume**

All manipulations were performed on ice. 1.5µl of cDNA were pipetted in each PCR tube. Then, GoTag polymerase was added to the Master Mix, which was carefully mixed. 23.5µl from the Master Mix were added to each sample. The total reaction volume was 25µl.

The PCR runs were performed using the GeneAmp PCR Systems (Applied Biosystems).

Protocol for PCR:

2’	95°C	
30’’	95°C	
30’’	55°C	] 25 cycles
1’	72°C	
7’	72°C	
∞	4°C	

The different samples were subsequently analyzed by Agarose Gel electrophoresis (see 2.2.4)

4.2.16 qRT-PCR

qRT-PCR was performed using SensiMix Plus SYBR Green reaction mix. Each sample contained approx. 10 ng cDNA dependent on how much cDNA was available. It is important, that every sample contained always the same amounts of cDNA. The sample volume was in the end 10 µl, of which 5.8µl were the Syber Green Primer master mix and 4.2 µl were the cDNA dilution.

cDNA dilution:

5 µl	DNA (100ng/µl)
195 µl	ddH2O
200 µl	total volume
→from this 4.2 µl (10.5ng DNA) in each sample	

The original cDNA have to be diluted, that in 4.2µl are approx. 10ng cDNA.

Syber Green Master mix for 1 sample:

5 µl	Syber Green
0.4 µl	Forward primer (4µM)
0.4 µl	Reverse primer (4µM)
5.8 µl	total volume

In each run 4 additional samples, called "standard dilutions", containing different dilutions of the cDNA (total cDNA amount: 20ng, 2ng, 0.2ng and 0.02ng) were included. These standard dilution values are indicated for each analysed gene and are used by the qRT-PCR machine to calculate the results of the samples. A "no template" control only containing nuclease free water and the "–RT" sample were included in each run. When all cDNA dilutions and Syber Green Primer Master mix were prepared, the cDNA was first equally distributed into the qPCR tubes (4.2µl in each tube) and then 5.8µl of the Syber Green Primer Master mix were added. All preparation was done one ice using the 72-well PCR plate. The PCR run was performed in the Rotor Gene (RG-300A) from Rcorbett Research and the manufactered instructions were followed.

Procedure of PCR:

Initial incubation	10 minutes	95°C	
Denature	20 seconds	95°C	⎫
Annealing	30 seconds	60°C	⎬ 40 cycles
Elongation	30 seconds	72°C	⎭
Melting curve	heating up from 60-99°C		

The fluorescence data were collected automatically after each cycle. A melt curve was calculated in the end by heating the samples from 60 to 99°C. The fluorescence data were analyzed by the Rotor-Gene computer program.

4.2.17 Agarose Gel electrophoresis

To analyze DNA samples after PCR reactions, agarose gel electrophoresis was performed. At physiological pH, DNA is an acidic molecule with each nucleotide carrying one negative charge at its phosphate group. For the separation of DNA fragments between 1 kbp and 10 kbp, a 1.5 % (w/v) agarose solution in 1x TAE buffer (70 ml for a small gel and 140 ml for a big gel) was prepared and heated in a microwave oven until the solution started to boil. Afterwards, the liquid agarose solution was poured into a gel tray in the cold room (4°C) and 5–10 µl ethidium bromide were added to the agarose solution. Ethidium bromide intercalates with doublestranded DNA and fluoresces when excised at 302 nm. A comb was inserted into the gel to form the sample pockets. After the gel had completely solidified, it was transferred into the electrophoresis unit and covered with 1x TAE buffer. The comb was removed and DNA samples, to which a tenth part of 10x DNA loading buffer was previously added, were loaded. A DNA marker was also loaded to one of the sample pockets as control. Typically, Phage lambda DNA digested with Pst, containing fragments from 250 to 10,000 base pairs, was used as marker. 5-10 µl ethidium bromide solution were added into 1x TAE buffer in the tank. Samples were allowed to enter the gel at a constant voltage of 80 V for 15 minutes. The voltage was then increased to 120 V and gels were run for another 20 minutes before being removed from the gel tray. The interaction of ethidium bromide with doublestranded DNA allowed the detection of DNA under UV light.

5 References

1. Hassa, P. O., and Hottiger, M. O. (2002) The functional role of poly(ADP-ribose)polymerase 1 as novel coactivator of NF-kappaB in inflammatory disorders. *Cell Mol Life Sci* 59, Page.
2. Hoffmann, A., Natoli, G., and Ghosh, G. (2006) Transcriptional regulation via the NF-kappaB signaling module. *Oncogene* 25, Page.
3. Ghosh, S., May, M. J., and Kopp, E. B. (1998) NF-kappa B and Rel proteins: evolutionarily conserved mediators of immune responses. *Annu Rev Immunol* 16, Page.
4. Sharif, O., Bolshakov, V. N., Raines, S., Newham, P., and Perkins, N. D. (2007) Transcriptional profiling of the LPS induced NF-kappaB response in macrophages. *BMC Immunol* 8, Page.
5. Perkins, N. D. (2007) Integrating cell-signalling pathways with NF-kappaB and IKK function. *Nat Rev Mol Cell Biol* 8, Page.
6. Karin, M. (1998) The NF-kappa B activation pathway: its regulation and role in inflammation and cell survival. *Cancer J Sci Am* 4 Suppl 1, Page.
7. Beg, A. A., and Baldwin, A. S., Jr. (1993) The I kappa B proteins: multifunctional regulators of Rel/NF-kappa B transcription factors. *Genes Dev* 7, Page.
8. Ghosh, S., and Hayden, M. S. (2008) New regulators of NF-kappaB in inflammation. *Nat Rev Immunol* 8, Page.
9. Scheidereit, C. (2006) IkappaB kinase complexes: gateways to NF-kappaB activation and transcription. *Oncogene* 25, Page.
10. Senftleben, U., Cao, Y., Xiao, G., Greten, F. R., Krahn, G., Bonizzi, G., Chen, Y., Hu, Y., Fong, A., Sun, S. C., and Karin, M. (2001) Activation by IKKalpha of a second, evolutionary conserved, NF-kappa B signaling pathway. *Science* 293, Page.
11. Hoffmann, A., Levchenko, A., Scott, M. L., and Baltimore, D. (2002) The IkappaB-NF-kappaB signaling module: temporal control and selective gene activation. *Science* 298, Page.
12. Werner, S. L., Barken, D., and Hoffmann, A. (2005) Stimulus specificity of gene expression programs determined by temporal control of IKK activity. *Science* 309, Page.
13. Han, J., and Ulevitch, R. J. (2005) Limiting inflammatory responses during activation of innate immunity. *Nat Immunol* 6, Page.
14. Hoffmann, A., Leung, T. H., and Baltimore, D. (2003) Genetic analysis of NF-kappaB/Rel transcription factors defines functional specificities. *EMBO J* 22, Page.
15. Akira, S., Takeda, K., and Kaisho, T. (2001) Toll-like receptors: critical proteins linking innate and acquired immunity. *Nat Immunol* 2, Page.
16. Kaisho, T., and Akira, S. (2000) Critical roles of Toll-like receptors in host defense. *Crit Rev Immunol* 20, Page.
17. Chambon, P., Weill, J. D., and Mandel, P. (1963) Nicotinamide mononucleotide activation of new DNA-dependent polyadenylic acid synthesizing nuclear enzyme. *Biochem Biophys Res Commun* 11, Page.
18. Kraus, W. L., and Lis, J. T. (2003) PARP goes transcription. *Cell* 113, Page.
19. Wang, Z. Q., Auer, B., Stingl, L., Berghammer, H., Haidacher, D., Schweiger, M., and Wagner, E. F. (1995) Mice lacking ADPRT and poly(ADP-ribosyl)ation develop normally but are susceptible to skin disease. *Genes Dev* 9, Page.

20. Shieh, W. M., Ame, J. C., Wilson, M. V., Wang, Z. Q., Koh, D. W., Jacobson, M. K., and Jacobson, E. L. (1998) Poly(ADP-ribose) polymerase null mouse cells synthesize ADP-ribose polymers. *J Biol Chem* 273, Page.
21. Ame, J. C., Rolli, V., Schreiber, V., Niedergang, C., Apiou, F., Decker, P., Muller, S., Hoger, T., Menissier-de Murcia, J., and de Murcia, G. (1999) PARP-2, A novel mammalian DNA damage-dependent poly(ADP-ribose) polymerase. *J Biol Chem* 274, Page.
22. Hassa, P. O., Haenni, S. S., Elser, M., and Hottiger, M. O. (2006) Nuclear ADP-ribosylation reactions in mammalian cells: where are we today and where are we going? *Microbiol Mol Biol Rev* 70, Page.
23. Schreiber, V., Dantzer, F., Ame, J. C., and de Murcia, G. (2006) Poly(ADP-ribose): novel functions for an old molecule. *Nat Rev Mol Cell Biol* 7, Page.
24. Ame, J. C., Spenlehauer, C., and de Murcia, G. (2004) The PARP superfamily. *Bioessays* 26, Page.
25. D'Amours, D., Desnoyers, S., D'Silva, I., and Poirier, G. G. (1999) Poly(ADP-ribosyl)ation reactions in the regulation of nuclear functions. *Biochem J* 342 (Pt 2), Page.
26. de Murcia, G., Schreiber, V., Molinete, M., Saulier, B., Poch, O., Masson, M., Niedergang, C., and Menissier de Murcia, J. (1994) Structure and function of poly(ADP-ribose) polymerase. *Mol Cell Biochem* 138, Page.
27. Gradwohl, G., Menissier de Murcia, J. M., Molinete, M., Simonin, F., Koken, M., Hoeijmakers, J. H., and de Murcia, G. (1990) The second zinc-finger domain of poly(ADP-ribose) polymerase determines specificity for single-stranded breaks in DNA. *Proc Natl Acad Sci U S A* 87, Page.
28. Ikejima, M., Noguchi, S., Yamashita, R., Ogura, T., Sugimura, T., Gill, D. M., and Miwa, M. (1990) The zinc fingers of human poly(ADP-ribose) polymerase are differentially required for the recognition of DNA breaks and nicks and the consequent enzyme activation. Other structures recognize intact DNA. *J Biol Chem* 265, Page.
29. Hilz, H., Wielckens, K., Adamietz, P., Bredehorst, R., and Kreymeier, A. (1983) Functional aspects of mono- and poly(ADP-ribosyl)ation: subcellular distribution and ADP-ribosyl turnover under conditions of repair and 'starvation'. *Princess Takamatsu Symp* 13, Page.
30. Alvarez-Gonzalez, R., Watkins, T. A., Gill, P. K., Reed, J. L., and Mendoza-Alvarez, H. (1999) Regulatory mechanisms of poly(ADP-ribose) polymerase. *Mol Cell Biochem* 193, Page.
31. Alvarez-Gonzalez, R., and Jacobson, M. K. (1987) Characterization of polymers of adenosine diphosphate ribose generated in vitro and in vivo. *Biochemistry* 26, Page.
32. Juarez-Salinas, H., Levi, V., Jacobson, E. L., and Jacobson, M. K. (1982) Poly(ADP-ribose) has a branched structure in vivo. *J Biol Chem* 257, Page.
33. Anderson, M. G., Scoggin, K. E., Simbulan-Rosenthal, C. M., and Steadman, J. A. (2000) Identification of poly(ADP-ribose) polymerase as a transcriptional coactivator of the human T-cell leukemia virus type 1 Tax protein. *J Virol* 74, Page.
34. Nie, J., Sakamoto, S., Song, D., Qu, Z., Ota, K., and Taniguchi, T. (1998) Interaction of Oct-1 and automodification domain of poly(ADP-ribose) synthetase. *FEBS Lett* 424, Page.
35. Hassa, P. O., and Hottiger, M. O. (1999) A role of poly (ADP-ribose) polymerase in NF-kappaB transcriptional activation. *Biol Chem* 380, Page.
36. Malanga, M., and Althaus, F. R. (2005) The role of poly(ADP-ribose) in the DNA damage signaling network. *Biochem Cell Biol* 83, Page.

37. Althaus, F. R. (1992) Poly ADP-ribosylation: a histone shuttle mechanism in DNA excision repair. *J Cell Sci* 102 (Pt 4), Page.
38. Realini, C. A., and Althaus, F. R. (1992) Histone shuttling by poly(ADP-ribosylation). *J Biol Chem* 267, Page.
39. Schreiber, V., Ame, J. C., Dolle, P., Schultz, I., Rinaldi, B., Fraulob, V., Menissier-de Murcia, J., and de Murcia, G. (2002) Poly(ADP-ribose) polymerase-2 (PARP-2) is required for efficient base excision DNA repair in association with PARP-1 and XRCC1. *J Biol Chem* 277, Page.
40. Huletsky, A., de Murcia, G., Muller, S., Hengartner, M., Menard, L., Lamarre, D., and Poirier, G. G. (1989) The effect of poly(ADP-ribosyl)ation on native and H1-depleted chromatin. A role of poly(ADP-ribosyl)ation on core nucleosome structure. *J Biol Chem* 264, Page.
41. Poirier, G. G., de Murcia, G., Jongstra-Bilen, J., Niedergang, C., and Mandel, P. (1982) Poly(ADP-ribosyl)ation of polynucleosomes causes relaxation of chromatin structure. *Proc Natl Acad Sci U S A* 79, Page.
42. Skidmore, C. J., Davies, M. I., Goodwin, P. M., Halldorsson, H., Lewis, P. J., Shall, S., and Zia'ee, A. A. (1979) The involvement of poly(ADP-ribose) polymerase in the degradation of NAD caused by gamma-radiation and N-methyl-N-nitrosourea. *Eur J Biochem* 101, Page.
43. Berger, N. A. (1985) Poly(ADP-ribose) in the cellular response to DNA damage. *Radiat Res* 101, Page.
44. Berger, N. A., Sims, J. L., Catino, D. M., and Berger, S. J. (1983) Poly(ADP-ribose) polymerase mediates the suicide response to massive DNA damage: studies in normal and DNA-repair defective cells. *Princess Takamatsu Symp* 13, Page.
45. Susin, S. A., Lorenzo, H. K., Zamzami, N., Marzo, I., Snow, B. E., Brothers, G. M., Mangion, J., Jacotot, E., Costantini, P., Loeffler, M., Larochette, N., Goodlett, D. R., Aebersold, R., Siderovski, D. P., Penninger, J. M., and Kroemer, G. (1999) Molecular characterization of mitochondrial apoptosis-inducing factor. *Nature* 397, Page.
46. Yu, S. W., Wang, H., Poitras, M. F., Coombs, C., Bowers, W. J., Federoff, H. J., Poirier, G. G., Dawson, T. M., and Dawson, V. L. (2002) Mediation of poly(ADP-ribose) polymerase-1-dependent cell death by apoptosis-inducing factor. *Science* 297, Page.
47. Chen, M., Zsengeller, Z., Xiao, C. Y., and Szabo, C. (2004) Mitochondrial-to-nuclear translocation of apoptosis-inducing factor in cardiac myocytes during oxidant stress: potential role of poly(ADP-ribose) polymerase-1. *Cardiovasc Res* 63, Page.
48. Kaufmann, S. H., Desnoyers, S., Ottaviano, Y., Davidson, N. E., and Poirier, G. G. (1993) Specific proteolytic cleavage of poly(ADP-ribose) polymerase: an early marker of chemotherapy-induced apoptosis. *Cancer Res* 53, Page.
49. Petrilli, V., Herceg, Z., Hassa, P. O., Patel, N. S., Di Paola, R., Cortes, U., Dugo, L., Filipe, H. M., Thiemermann, C., Hottiger, M. O., Cuzzocrea, S., and Wang, Z. Q. (2004) Noncleavable poly(ADP-ribose) polymerase-1 regulates the inflammation response in mice. *J Clin Invest* 114, Page.
50. Carbone, M., Rossi, M. N., Cavaldesi, M., Notari, A., Amati, P., and Maione, R. (2008) Poly(ADP-ribosyl)ation is implicated in the G0-G1 transition of resting cells. *Oncogene* 27, Page.
51. de Murcia, J. M., Niedergang, C., Trucco, C., Ricoul, M., Dutrillaux, B., Mark, M., Oliver, F. J., Masson, M., Dierich, A., LeMeur, M., Walztinger, C., Chambon, P., and de Murcia, G. (1997) Requirement of poly(ADP-ribose) polymerase in recovery from DNA damage in mice and in cells. *Proc Natl Acad Sci U S A* 94, Page.
52. Masutani, M., Nozaki, T., Nishiyama, E., Shimokawa, T., Tachi, Y., Suzuki, H., Nakagama, H., Wakabayashi, K., and Sugimura, T. (1999) Function of poly(ADP-

ribose) polymerase in response to DNA damage: gene-disruption study in mice. *Mol Cell Biochem* 193, Page.
53. Shall, S., and de Murcia, G. (2000) Poly(ADP-ribose) polymerase-1: what have we learned from the deficient mouse model? *Mutat Res* 460, Page.
54. Pieper, A. A., Brat, D. J., Krug, D. K., Watkins, C. C., Gupta, A., Blackshaw, S., Verma, A., Wang, Z. Q., and Snyder, S. H. (1999) Poly(ADP-ribose) polymerase-deficient mice are protected from streptozotocin-induced diabetes. *Proc Natl Acad Sci U S A* 96, Page.
55. Burkart, V., Wang, Z. Q., Radons, J., Heller, B., Herceg, Z., Stingl, L., Wagner, E. F., and Kolb, H. (1999) Mice lacking the poly(ADP-ribose) polymerase gene are resistant to pancreatic beta-cell destruction and diabetes development induced by streptozocin. *Nat Med* 5, Page.
56. Soriano, F. G., Virag, L., and Szabo, C. (2001) Diabetic endothelial dysfunction: role of reactive oxygen and nitrogen species production and poly(ADP-ribose) polymerase activation. *J Mol Med* 79, Page.
57. Szabo, C., Lim, L. H., Cuzzocrea, S., Getting, S. J., Zingarelli, B., Flower, R. J., Salzman, A. L., and Perretti, M. (1997) Inhibition of poly (ADP-ribose) synthetase attenuates neutrophil recruitment and exerts antiinflammatory effects. *J Exp Med* 186, Page.
58. Oliver, F. J., Menissier-de Murcia, J., Nacci, C., Decker, P., Andriantsitohaina, R., Muller, S., de la Rubia, G., Stoclet, J. C., and de Murcia, G. (1999) Resistance to endotoxic shock as a consequence of defective NF-kappaB activation in poly (ADP-ribose) polymerase-1 deficient mice. *EMBO J* 18, Page.
59. Liaudet, L., Pacher, P., Mabley, J. G., Virag, L., Soriano, F. G., Hasko, G., and Szabo, C. (2002) Activation of poly(ADP-Ribose) polymerase-1 is a central mechanism of lipopolysaccharide-induced acute lung inflammation. *Am J Respir Crit Care Med* 165, Page.
60. Mabley, J. G., Jagtap, P., Perretti, M., Getting, S. J., Salzman, A. L., Virag, L., Szabo, E., Soriano, F. G., Liaudet, L., Abdelkarim, G. E., Hasko, G., Marton, A., Southan, G. J., and Szabo, C. (2001) Anti-inflammatory effects of a novel, potent inhibitor of poly (ADP-ribose) polymerase. *Inflamm Res* 50, Page.
61. Eliasson, M. J., Sampei, K., Mandir, A. S., Hurn, P. D., Traystman, R. J., Bao, J., Pieper, A., Wang, Z. Q., Dawson, T. M., Snyder, S. H., and Dawson, V. L. (1997) Poly(ADP-ribose) polymerase gene disruption renders mice resistant to cerebral ischemia. *Nat Med* 3, Page.
62. Kuhnle, S., Nicotera, P., Wendel, A., and Leist, M. (1999) Prevention of endotoxin-induced lethality, but not of liver apoptosis in poly(ADP-ribose) polymerase-deficient mice. *Biochem Biophys Res Commun* 263, Page.
63. Jagtap, P., and Szabo, C. (2005) Poly(ADP-ribose) polymerase and the therapeutic effects of its inhibitors. *Nat Rev Drug Discov* 4, Page.
64. Menissier de Murcia, J., Ricoul, M., Tartier, L., Niedergang, C., Huber, A., Dantzer, F., Schreiber, V., Ame, J. C., Dierich, A., LeMeur, M., Sabatier, L., Chambon, P., and de Murcia, G. (2003) Functional interaction between PARP-1 and PARP-2 in chromosome stability and embryonic development in mouse. *EMBO J* 22, Page.
65. Tsutsumi, M., Masutani, M., Nozaki, T., Kusuoka, O., Tsujiuchi, T., Nakagama, H., Suzuki, H., Konishi, Y., and Sugimura, T. (2001) Increased susceptibility of poly(ADP-ribose) polymerase-1 knockout mice to nitrosamine carcinogenicity. *Carcinogenesis* 22, Page.
66. Tong, W. M., Ohgaki, H., Huang, H., Granier, C., Kleihues, P., and Wang, Z. Q. (2003) Null mutation of DNA strand break-binding molecule poly(ADP-ribose) polymerase causes medulloblastomas in p53(-/-) mice. *Am J Pathol* 162, Page.

67. Conde, C., Mark, M., Oliver, F. J., Huber, A., de Murcia, G., and Menissier-de Murcia, J. (2001) Loss of poly(ADP-ribose) polymerase-1 causes increased tumour latency in p53-deficient mice. *EMBO J* 20, Page.
68. Martin-Oliva, D., Aguilar-Quesada, R., O'Valle, F., Munoz-Gamez, J. A., Martinez-Romero, R., Garcia Del Moral, R., Ruiz de Almodovar, J. M., Villuendas, R., Piris, M. A., and Oliver, F. J. (2006) Inhibition of poly(ADP-ribose) polymerase modulates tumor-related gene expression, including hypoxia-inducible factor-1 activation, during skin carcinogenesis. *Cancer Res* 66, Page.
69. Klosterhalfen, B., and Bhardwaj, R. S. (1998) Septic shock. *Gen Pharmacol* 31, Page.
70. Beutler, B., and Poltorak, A. (2001) Sepsis and evolution of the innate immune response. *Crit Care Med* 29, Page.
71. Fink, M. P., and Heard, S. O. (1990) Laboratory models of sepsis and septic shock. *J Surg Res* 49, Page.
72. Downey, J. S., and Han, J. (1998) Cellular activation mechanisms in septic shock. *Front Biosci* 3, Page.
73. Szabo, C., Cuzzocrea, S., Zingarelli, B., O'Connor, M., and Salzman, A. L. (1997) Endothelial dysfunction in a rat model of endotoxic shock. Importance of the activation of poly (ADP-ribose) synthetase by peroxynitrite. *J Clin Invest* 100, Page.
74. Perkins, N. D. (2000) The Rel/NF-kappa B family: friend and foe. *Trends Biochem Sci* 25, Page.
75. Mattson, M. P., and Camandola, S. (2001) NF-kappaB in neuronal plasticity and neurodegenerative disorders. *J Clin Invest* 107, Page.
76. Hassa, P. O., Covic, M., Hasan, S., Imhof, R., and Hottiger, M. O. (2001) The enzymatic and DNA binding activity of PARP-1 are not required for NF-kappa B coactivator function. *J Biol Chem* 276, Page.
77. Ha, H. C., Hester, L. D., and Snyder, S. H. (2002) Poly(ADP-ribose) polymerase-1 dependence of stress-induced transcription factors and associated gene expression in glia. *Proc Natl Acad Sci U S A* 99, Page.
78. Perkins, N. D., Felzien, L. K., Betts, J. C., Leung, K., Beach, D. H., and Nabel, G. J. (1997) Regulation of NF-kappaB by cyclin-dependent kinases associated with the p300 coactivator. *Science* 275, Page.
79. Lodish (2002) *Molecular Cell Biology*, 4th Ed.
80. Dehay, C., and Kennedy, H. (2007) Cell-cycle control and cortical development. *Nat Rev Neurosci* 8, Page.
81. Vadiveloo, P. K. (1999) Macrophages--proliferation, activation, and cell cycle proteins. *J Leukoc Biol* 66, Page.
82. Merrill, G. F. (1998) Cell synchronization. *Methods Cell Biol* 57, Page.
83. Cooper, S. (2003) Rethinking synchronization of mammalian cells for cell cycle analysis. *Cell Mol Life Sci* 60, Page.
84. Schorl, C., and Sedivy, J. M. (2007) Analysis of cell cycle phases and progression in cultured mammalian cells. *Methods* 41, Page.
85. Barre, B., and Perkins, N. D. (2007) A cell cycle regulatory network controlling NF-kappaB subunit activity and function. *EMBO J* 26, Page.
86. Shanmugham, L. N., Petrarca, C., Frydas, S., Donelan, J., Castellani, M. L., Boucher, W., Madhappan, B., Tete, S., Falasca, K., Conti, P., and Vecchiet, J. (2006) IL-15 an immunoregulatory and anti-cancer cytokine. Recent advances. *J Exp Clin Cancer Res* 25, Page.
87. Ju, B. G., Solum, D., Song, E. J., Lee, K. J., Rose, D. W., Glass, C. K., and Rosenfeld, M. G. (2004) Activating the PARP-1 sensor component of the groucho/ TLE1 corepressor complex mediates a CaMKinase IIdelta-dependent neurogenic gene activation pathway. *Cell* 119, Page.

88. Gagne, J. P., Moreel, X., Gagne, P., Labelle, Y., Droit, A., Chevalier-Pare, M., Bourassa, S., McDonald, D., Hendzel, M. J., Prigent, C., and Poirier, G. G. (2008) Proteomic Investigation of Phosphorylation Sites in Poly(ADP-ribose) Polymerase-1 and Poly(ADP-ribose) Glycohydrolase. *J Proteome Res*, Page.
89. Yamamoto, Y., and Gaynor, R. B. (2001) Therapeutic potential of inhibition of the NF-kappaB pathway in the treatment of inflammation and cancer. *J Clin Invest* 107, Page.

6 Curriculum Vitae

Name:	Bäckert
Vorname:	Sandra Manuela
Geburtsdatum:	13. September 1984
Heimatort:	Riehen BS

Ausbildung:

1991 – 1996	Primarschule Dornach
1996 – 2000	Progymnasium Reinach
2000 – 2003	Gymnasium Münchenstein Matura Schwerpunkt Biologie und Chemie (2003)
2004 – 2009	Veterinärmedizin Studium an der Vetsuisse Fakultät der Universität Zürich mit Schwerpunkt Biomedizinische Forschung
2008 – 2009	Dissertation am Institut für Veterinärbiochemie und Molekularbiologie an der Vetsuisse Fakultät der Universität Zürich

7 Acknowledgements

My greatest thank is dedicated to Prof. Dr. Michael O. Hottiger who gave me the opportunity to do my thesis in his lab. Thanks very much for the guidance, patience and support.

A big thank goes to Matthias Altmeyer, he was my supervisor in the laboratory, personal helpdesk and good friend at the same time. He learned me everything about molecular biology, teached me how to perform experiments, was always there when I needed some help, had a huge patience to listen to all my problems and always helped me to solve them.

Furthermore I would like to highly acknowledge the help of the whole Hottiger group. Moni, Karin, Sandrine, Simone, Suheda and Ingrid were always there when I needed some instructions for the lab work, when I was looking for something or when I needed a discussion partner to solve my problems. I would like to thank them all for their great help, support and the friendly atmosphere in the lab.

I would also like to acknowledge all the other members of the Institute for the friendly working environment.

Last, but definitively not least I want to thank the people in my private environment. I am deeply indebted to my family for their emotional and financial support over the last years. Without them I would not be where I am today. And I would also like to thank my mother to take care about Tosca and Simba.

Also friends should not go unnoticed. Most important I would like to express my deep gratitude to Jan Kristian Larsen for his shoulder to lie on, patience, support, tolerance and love.